REPORT

www.the-innovation.org

Alzheimer's disease early diagnostic and staging biomarkers revealed by large-scale cerebrospinal fluid and serum proteomic profiling

Qing-Qing Tao,[1,2,10] Xue Cai,[3,4,10] Yan-Yan Xue,[1,10] Weigang Ge,[3,4,10] Liang Yue,[3,4] Xiao-Yan Li,[1] Rong-Rong Lin,[1] Guo-Ping Peng,[5] Wenhao Jiang,[3,4] Sainan Li,[3,4] Kun-Mu Zheng,[6] Bin Jiang,[6] Jian-Ping Jia,[7,*] Tiannan Guo,[3,4,*] and Zhi-Ying Wu[1,2,8,9,*]

*Correspondence: jpjia@ccmu.edu.cn (J.-P.J.); guotiannan@westlake.edu.cn (T.G.); zhiyingwu@zju.edu.cn (Z.-Y.W.)

Received: June 12, 2023; Accepted: November 19, 2023; Published Online: January 2, 2024; https://doi.org/10.1016/j.xinn.2023.100544

GRAPHICAL ABSTRACT

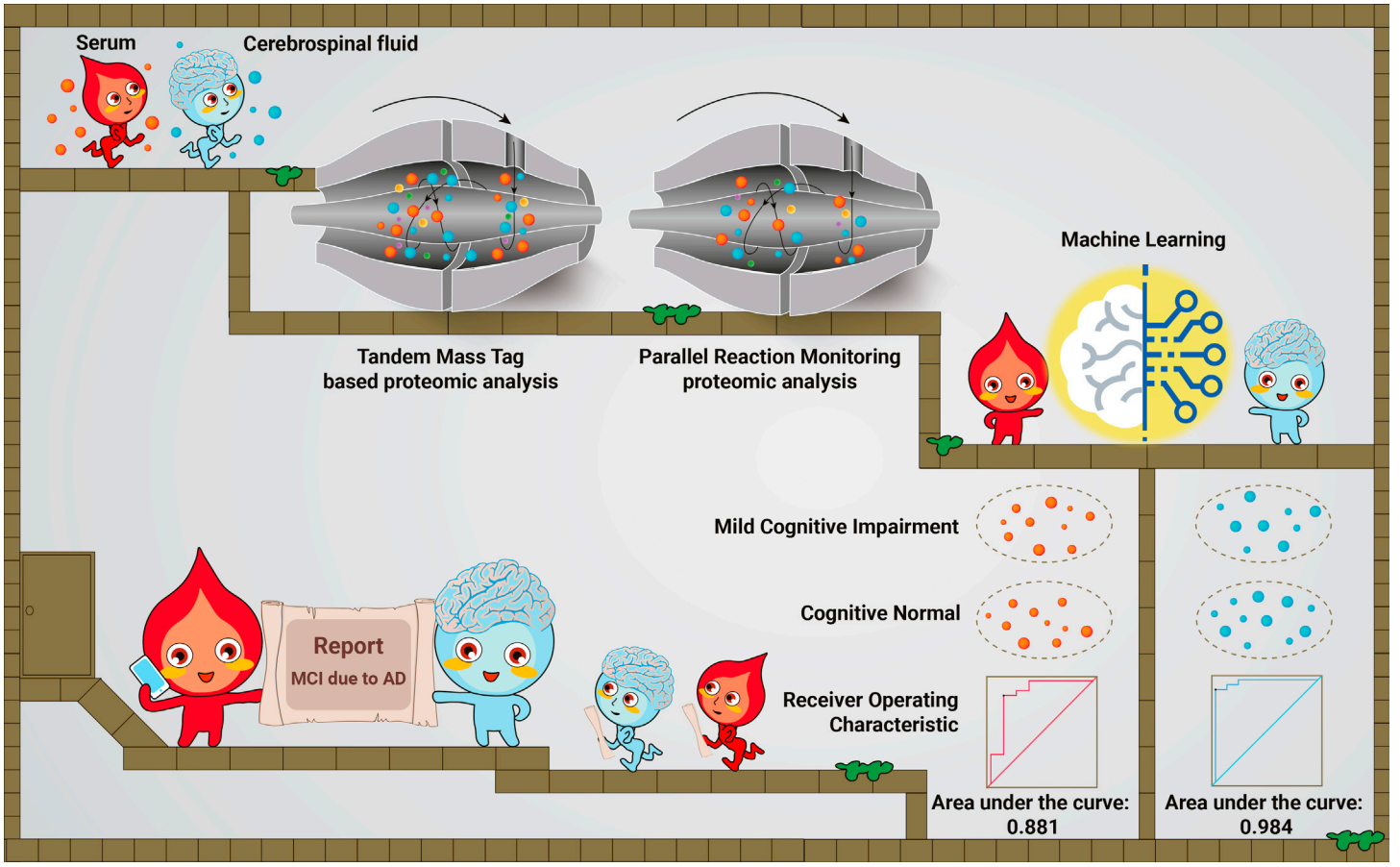

PUBLIC SUMMARY

- In-depth proteomics workflow for profiling paired cerebrospinal fluid (CSF) and serum proteomes.
- Independent multicenter set combined with multiple methods for validation.
- Development of 19 CSF- and 8 serum-protein panels for early of Alzheimer disease (AD) diagnosis.
- Twenty-one CSF and 18 serum proteins dysregulated in different AD stages.
- Groundwork laid for AD blood tests in clinical screening and staging.

REPORT

Alzheimer's disease early diagnostic and staging biomarkers revealed by large-scale cerebrospinal fluid and serum proteomic profiling

Qing-Qing Tao,[1,2,10] Xue Cai,[3,4,10] Yan-Yan Xue,[1,10] Weigang Ge,[3,4,10] Liang Yue,[3,4] Xiao-Yan Li,[1] Rong-Rong Lin,[1] Guo-Ping Peng,[5] Wenhao Jiang,[3,4] Sainan Li,[3,4] Kun-Mu Zheng,[6] Bin Jiang,[6] Jian-Ping Jia,[7,*] Tiannan Guo,[3,4,*] and Zhi-Ying Wu[1,2,8,9,*]

[1]Department of Neurology and Research Center of Neurology in the Second Affiliated Hospital and Key Laboratory of Medical Neurobiology of Zhejiang Province, Zhejiang University School of Medicine, Hangzhou 310009, China

[2]Liangzhu Laboratory, Zhejiang University, Hangzhou 311100, China

[3]Westlake Laboratory of Life Sciences and Biomedicine, Key Laboratory of Structural Biology of Zhejiang Province, School of Life Sciences, Westlake University, Hangzhou 310024, China

[4]Institute of Basic Medical Sciences, Westlake Institute for Advanced Study, Hangzho 310024, China

[5]Department of Neurology, First Affiliated Hospital, Zhejiang University School of Medicine, Hangzhou 310009, China

[6]Department of Neurology, First Affiliated Hospital, School of Medicine, Xiamen University, Xiamen 361009, China

[7]Innovation Center for Neurological Disorders and Department of Neurology, Xuanwu Hospital, Capital Medical University, National Clinical Research Center for Geriatric Diseases, Beijing 100053, China

[8]MOE Frontier Science Center for Brain Science and Brain-machine Integration, School of Brain Science and Brain Medicine, Zhejiang University, Hangzhou 310058, China

[9]CAS Center for Excellence in Brain Science and Intelligence Technology, Shanghai 200031, China

[10]These authors contributed equally

*Correspondence: jpjia@ccmu.edu.cn (J.-P.J.); guotiannan@westlake.edu.cn (T.G.); zhiyingwu@zju.edu.cn (Z.-Y.W.)

Received: June 12, 2023; Accepted: November 19, 2023; Published Online: January 2, 2024; https://doi.org/10.1016/j.xinn.2023.100544

Citation: Tao Q.-Q., Cai X., Xue Y.-Y., et al., (2024). Alzheimer's disease early diagnostic and staging biomarkers revealed by large-scale cerebrospinal fluid and serum proteomic profiling. The Innovation **5(1)**, 100544.

Amyloid-β, tau pathology, and biomarkers of neurodegeneration make up the core diagnostic biomarkers of Alzheimer disease (AD). However, these proteins represent only a fraction of the complex biological processes underlying AD, and individuals with other brain diseases in which AD pathology is a comorbidity also test positive for these diagnostic biomarkers. More AD-specific early diagnostic and disease staging biomarkers are needed. In this study, we performed tandem mass tag proteomic analysis of paired cerebrospinal fluid (CSF) and serum samples in a discovery cohort comprising 98 participants. Candidate biomarkers were validated by parallel reaction monitoring–based targeted proteomic assays in an independent multicenter cohort comprising 288 participants. We quantified 3,238 CSF and 1,702 serum proteins in the discovery cohort, identifying 171 and 860 CSF proteins and 37 and 323 serum proteins as potential early diagnostic and staging biomarkers, respectively. In the validation cohort, 58 and 21 CSF proteins, as well as 12 and 18 serum proteins, were verified as early diagnostic and staging biomarkers, respectively. Separate 19-protein CSF and an 8-protein serum biomarker panels were built by machine learning to accurately classify mild cognitive impairment (MCI) due to AD from normal cognition with areas under the curve of 0.984 and 0.881, respectively. The 19-protein CSF biomarker panel also effectively discriminated patients with MCI due to AD from patients with other neurodegenerative diseases. Moreover, we identified 21 CSF and 18 serum stage-associated proteins reflecting AD stages. Our findings provide a foundation for developing blood-based tests for AD screening and staging in clinical practice.

INTRODUCTION

Alzheimer disease (AD) is the most common type of neurodegenerative disease and is pathologically characterized by the deposition of extracellular amyloid-β (Aβ) plaques and intracellular neurofibrillary tangles.[1] AD patients typically present with progressive cognitive decline. Extensive efforts have been made to determine the optimal strategy for diagnosing this devastating disease.[2–4] A research framework defining AD on the basis of Aβ deposition, phosphorylated tau (p-tau), and neurodegeneration was proposed in 2018.[5] However, positivity in these diagnostic biomarkers can also be observed in individuals with other brain diseases in which AD pathology has been recognized a comorbidity.[6] Furthermore, several limitations, such as high cost, insufficient accessibility, and invasiveness, impede the use of cerebrospinal fluid (CSF) and positron emission tomography (PET) biomarkers as first-line diagnostic strategies.

Blood testing is advantageous due to its convenience, minimal invasiveness, and affordability. Recently, several blood-based AD biomarkers, such as the plasma $A\beta_{42}/_{40}$ ratio, p-tau, neurofilament light polypeptide (NEFL), and glial fibrillary acidic protein (GFAP), have been reported.[7,8] Notably, plasma tau phosphorylated at threonine 217 (p-tau_{217}) could be used to accurately determine AD and was correlated with Aβ and p-tau pathology in the brain.[9] Nevertheless, plasma biomarkers for Aβ and tau pathology are not currently recommended for use in clinical practice because they remain to be further standardized and validated.[6] In addition, these clinical manifestations lose their correlation with both Aβ and p-tau protein levels as the disease progresses, suggesting that Aβ and p-tau biomarkers are not suitable for staging.[10] Converging findings indicate the presence of many additional pathological mechanisms underlying the pathogenesis of AD that are independent of Aβ and p-tau pathology.[11] Comprehensive research is necessary to identify early diagnostic and staging biomarkers for AD. We previously used proteomic analyses to identify blood biomarkers for evaluating the severity of coronavirus disease 2019.[12] In recent years, several mass spectrometry (MS)–based proteomics profiling studies of CSF and plasma have revealed protein biomarkers and insights into the biological processes underlying AD, with minimum sample amounts and high-throughput workflows.[2,13–16] However, early diagnostic and staging blood-based biomarkers of AD remain incompletely defined.

To systemically identify early diagnostic and staging biomarkers of AD, we performed high-throughput MS-based proteomics analysis in a discovery cohort with paired CSF and serum samples and validated the results in an independent multicenter validation cohort.

RESULTS

Study design

The study design is outlined in Figure 1. To explore early diagnostic and staging biomarkers of AD, we performed tandem mass tag (TMT)–based proteomic analysis of paired CSF and serum samples in the discovery cohort (Figure 1A; Table S1). We achieved a robust workflow with high proteome depth, quantifying 3,238 CSF (Figure S1) and 1,702 serum proteins (Figure S2; Table S2). The ranking of the median abundance of CSF proteins is shown in Figure S3A, and the identification depth of serum proteins is shown in Figure S3B. After filtering out proteins with a missing rate higher than 80%, 2,461 CSF proteins and 1,330 serum proteins remained for subsequent data analysis. The missing values of the two protein matrices were both 0.19. Potential early diagnosis and staging biomarkers in CSF and serum were determined. Mfuzz analysis was used to cluster the proteins that were dysregulated during the different stages of AD.[17] Then, the identified specific dysregulated proteins that differed between the cognitive normal (CN) group and mild cognitive impairment (MCI) due to AD group, as well as stage-dependent dysregulated proteins, were further validated in an independent multicenter cohort (Figure 1B). Machine learning models were built to classify MCI due to AD patients from CN participants. In addition, a cluster of CSF and serum proteins that were dysregulated in an AD stage–dependent manner was validated.

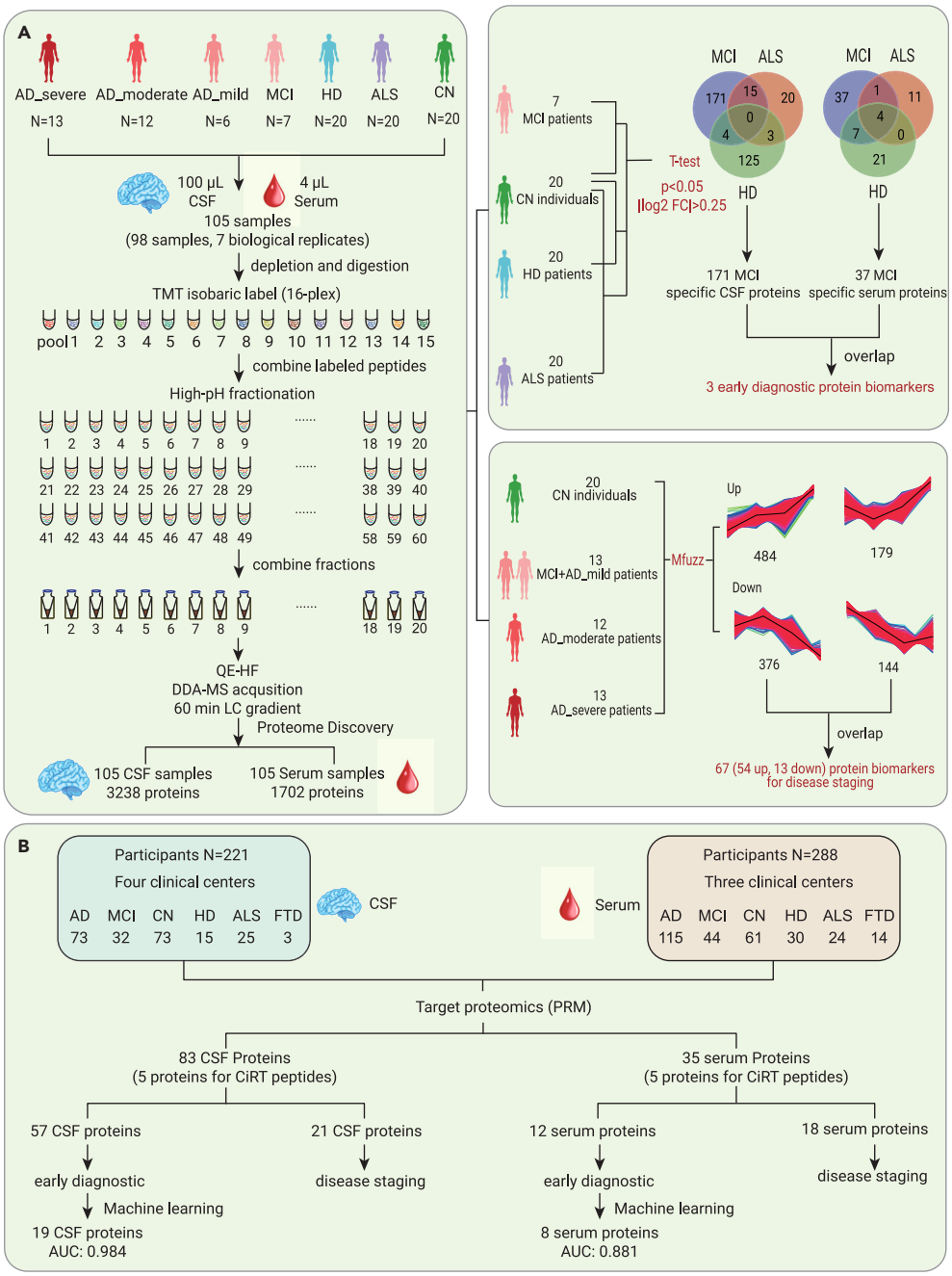

Figure 1. Overview of the study populations and schematic of the proteomic workflow (A) The workflow of the TMT-based proteome for the discovery of potential early AD diagnostic and staging biomarkers. Paired CSF and serum samples were collected from the discovery cohort, comprising patients with AD, MCI due to AD, HD, and ALS and CN participants. (B) The workflow of targeted proteomics for validating the early AD diagnostic and staging biomarkers. CSF and serum samples were collected from the validation cohort, comprising AD patients, patients with MCI due to AD, CN participants, and HD, ALS, and FTD patients.

TMT-based MS proteomics reveals proteins significantly altered in MCI due to AD

To identify the early CSF diagnostic biomarkers of AD, we compared the CSF proteomes of the MCI due to AD and CN participants in the discovery cohort. Compared with those of CN participants, the expression levels of 185 CSF proteins were upregulated ($p < 0.05$, log2 fold change [FC] > 0.25), and those of 5 CSF proteins were downregulated ($p < 0.05$, log2 FC <−0.25). To improve the specificity of the biomarkers, dysregulated proteins between CN and amyotrophic lateral sclerosis (ALS)/Huntington disease (HD) were excluded. The remaining 171 dysregulated proteins, including 167 with upregulated expression levels and 4 with downregulated expression levels, were CSF-specific biomarkers for MCI due to AD and were used for further validation (Figure 2A).

The 190 significantly dysregulated CSF proteins were analyzed using ingenuity pathway analysis (IPA) to identify enriched pathways. IPA showed molecular changes in the CSF of MCI due to AD patients relative to CN participants, implicating significant dysregulation (−log10 p > 1.3) of insulin growth factor 1 (IGF-1) signaling, dermatan sulfate biosynthesis, chondroitin sulfate biosynthesis, matrix metalloproteases, xenobiotic metabolism/pregnane X receptor (PXR), the constitutive androstane receptor (CAR) signaling pathway, heparan sulfate biosynthesis, and others, as shown in Figure 2B. Notably, we found that several identified pathways were closely related to the extracellular matrix (ECM; i.e., dermatan sulfate biosynthesis, chondroitin sulfate biosynthesis, and matrix metalloproteases). Our results imply the critical role of abnormal ECM metabolism in the pathogenesis of AD. In addition, several key dysregulated proteins in the CSF involved in these pathways are shown in Figure 2C.

To identify the blood-based early diagnostic biomarkers of AD, we analyzed the paired serum proteomes in the above participants. We identified 49 dysregulated proteins ($p < 0.05$, |log2 FC| > 0.25) between the MCI due to AD group and CN group. After excluding dysregulated serum proteins overlapping with the HD and ALS groups, 37 potential specific serum biomarkers for MCI due to AD were selected for further validation (Figure 2D).

In addition, IPA was used to analyze the 49 significantly dysregulated proteins to identify enriched pathways. The results showed molecular differences in the serum between the MCI due to AD patients and the CN group involving the following pathways: retinoate biosynthesis; the human leukocyte antigen-F adjacent transcript 10 cancer signaling pathway, natural killer cell signaling, the HOX transcript antisense RNA regulatory pathway, dendritic cell maturation, and others, as shown in Figure 2E. Several key dysregulated proteins involved in these pathways in MCI due to AD are shown in Figure 2F.

Verification of differentially expressed proteins in MCI due to AD in the independent validation cohort

To verify the results of the TMT-based proteomic analysis, a parallel reaction monitoring (PRM)-based targeted proteomic experiment was performed in an independent multicenter cohort. The validation cohort comprised 221 participants with CSF samples and 288 participants with serum samples (Figure 1B; Table S3). A total of 57 and 12 dysregulated CSF and serum proteins in the MCI due to AD group were verified, respectively (Table S4). In addition, we conducted real-time PCR to validate the transcription level of the differentially expressed proteins using the cortexes of 5×FAD mice. Two important candidates (GFAP and GM2A) were selected and verified (Figure S4).

We next explored the possibility of distinguishing between MCI due to AD and CN based on the dysregulated proteins. We formulated a random forest machine learning model using CSF proteomic data from 21 MCI due to AD and 52 CN participants. To ascertain the smallest number of proteins required to sufficiently differentiate MCI due to AD from CN, the prioritization of dysregulated proteins was explored by machine learning. A panel was constructed comprising the 19 proteins that were determined as

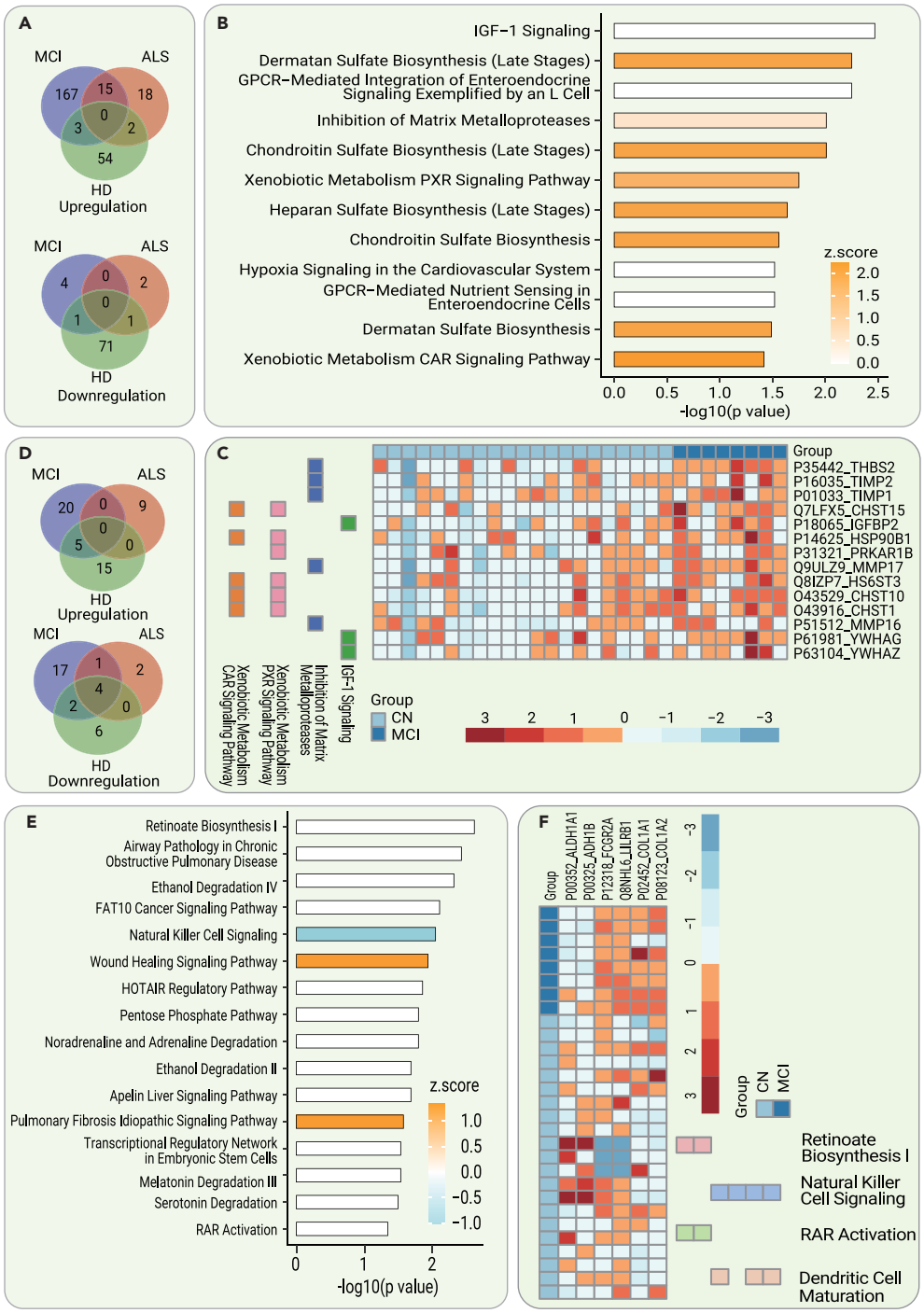

Figure 2. Dysregulated CSF and serum proteins and pathways in the diagnosis of early AD (A) Dysregulated ($p < 0.05$, $|\log2\ FC| > 0.25$) CSF proteins between MCI due to AD, ALS, and HD patients and CN participants. (B) The significantly dysregulated pathways ($-\log_{10} p > 1.3$) enriched by IPA using 190 dysregulated CSF proteins. (C) Heatmap of key dysregulated CSF proteins in various associated pathways in patients relative to CN participants. (D) Dysregulated ($p < 0.05$, $|\log2\ FC| > 0.25$) serum proteins between MCI due to AD, ALS, and HD patients and CN participants. (E) The significantly dysregulated pathways ($-\log10\ p > 1.3$) enriched by IPA using 49 dysregulated CSF proteins. (F) Heatmap of key dysregulated serum proteins in various associated pathways in patients relative to CN participants.

CSF early diagnostic biomarkers (Figure 3A). The abundance ranking of the 19 proteins among the identified CSF proteins in this study can be seen in Figure S3A. We then tested the model on 9 MCI due to AD and 21 CN participants. This model demonstrated a high level of accuracy, with an area under the curve (AUC) of 0.984 in the test set (Figure 3B). The classifier model had similar accuracy when stratifying by sex, age, or *APOE* ε4 genotype. Moreover, the 19-protein CSF biomarker panel could effectively discriminate MCI due to AD patients from frontotemporal dementia (FTD), ALS, and HD patients (Figure S5A).

Most of the selected proteins showed the same expression tendency in the discovery cohort and validation cohort that were assayed by the TMT and PRM experiments, respectively (Figure 3C). Notably, four (MGAT2, GM2A, MAN1C1, and MAN2A2) of the 19 proteins were related to the Golgi and lysosome pathways (i.e., function as enzymes or participate in the transport process to the Golgi). It is well known that pathways related to the Golgi apparatus and lysosomes have critical roles in the pathogenesis of neurodegenerative diseases such as AD, Parkinson disease (PD), and ALS.[18] The expression levels of all four proteins were upregulated in the MCI due to AD group relative to the CN group, suggesting that compensatory mechanisms may be initiated during the early stage of AD to protect against protein misfolding and aggregation. Among the 19 proteins in the panel, PCDHGC5 and IGHM are related to immune function (Figure 3C). IGHM has been reported to have an inverse correlation with Aβ burden in an AD mouse model.[19] Our data further supported the underlying connections between Aβ pathobiology and immunoglobulins.

Concomitantly, a random forest machine learning model was constructed based on the serum proteomic data from 23 participants with MCI due to AD and 45 CN participants. A panel consisting of 8 core proteins was selected to distinguish MCI due to AD from CN (Figure 4A). The rankings of the concentrations of these 8 proteins in the blood can be seen in Figure S3B. A cohort of 8 MCI due to AD and 21 CN participants was used to test the model, achieving an AUC of 0.881 (Figure 4B). The expression levels of 5 representative proteins with high confidence in the panel are shown in boxplots (Figure 4C). However, the ability to discriminate MCI due to AD from FTD, ALS, and HD was relatively low using the 8-protein serum biomarker panel (Figure S5B), which indicates that this analysis needs to be optimized further.

Subsequently, we proceeded to analyze the diagnostic efficiency for MCI due to AD based on the levels of serum GFAP and NEFL detected by commercially available Single Molecular Immunity Detection kits in a subset of the validation cohort, comprising 41 MCI due to AD patients, 14 FTD patients, 14 ALS patients, and 31 CN controls (Table S5). Compared to those of the CN controls, elevated levels of GFAP and NEFL were found in the sera of patients with ALS and FTD. In addition, patients with MCI due to AD exhibited increased levels of GFAP (Figure S6A). Receiver operating characteristic (ROC) curve analysis was used to evaluate the efficacy of serum GFAP, NEFL, and their combination in distinguishing between MCI due to AD participants and CN controls. The findings revealed that serum GFAP achieved an AUC of 0.714, whereas NEFL achieved an AUC of 0.511 (Figure S6B). In contrast to the two established serum biomarkers, our biomarker panel demonstrated superior diagnostic efficacy, with an AUC of 0.881. In addition, the levels of GFAP and NEFL were insufficient in differentiating patients with MCI due to AD from those with FTD and ALS (Figure S6C).

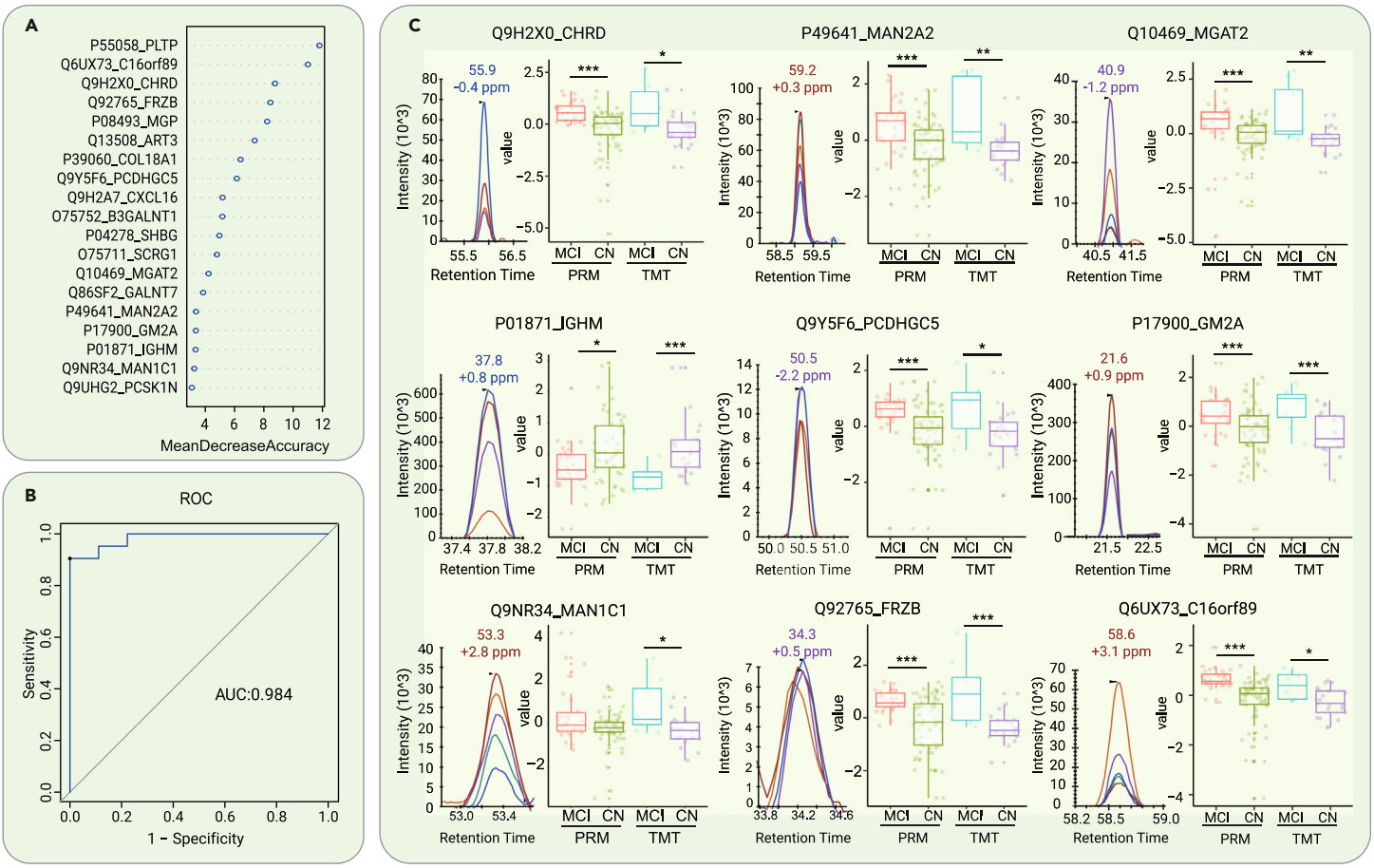

Figure 3. Differentiation of MCI due to AD and CN subjects by machine learning of CSF proteomic features (A) Top 19 proteins prioritized by random forest analysis ranked by the mean decrease in accuracy. (B) ROC curve of the random forest model. (C) Expression level change (*Z* scored original value) of 8 core proteins with significant differences between patients with MCI due to AD and CN participants in both TMT-based and PRM proteomic analyses. $p < 0.05$; $^{**}p < 0.01$; $^{***}p < 0.005$.

Correlations between the levels of core CSF and serum dysregulated proteins and the CSF levels of $A\beta_{42}$, t-tau, and p-tau_{181} in patients with MCI due to AD

We then explored whether the levels of the core dysregulated CSF and serum proteins in patients with MCI due to AD were correlated with the levels of CSF $A\beta_{42}$, t-tau, and p-tau_{181}. Interestingly, we found that among the 19 core CSF early diagnostic biomarkers, the levels of 2 (CHRD and COL18A1) were correlated with the levels of CSF $A\beta_{42}$, the levels of 4 others (B3GALNT1, GM2A, SHBG, and IGHM) were correlated with the levels of CSF p-tau_{181}, and the levels of yet 2 others (MAN2A2 and PCDHGC5) were correlated with the levels of both CSF $A\beta_{42}$ and p-tau_{181} (Figure S7). Among the 8 core serum early diagnostic biomarkers, C4B levels were correlated with CSF $A\beta_{42}$ levels, IGHV3-35 levels were correlated with CSF t-tau levels, and SERPINA11 levels were correlated with both CSF t-tau and p-tau_{181} levels (Figure S7). These results showed that only a fraction of the core dysregulated proteins we identified, 8/19 in CSF and 3/8 in serum, were associated with Aβ and p-tau pathology. This implies that the progression of AD is influenced by a variety of molecular pathways in addition to Aβ and p-tau.

Paired CSF and serum proteomes reveal proteins that are significantly altered during the progression of AD

To identify AD staging biomarkers, we compared the dysregulated proteins identified during the different stages of AD, including the MCI due to AD mild stage (ADM), AD moderate stage (ADMO), and AD severe stage (ADS). A total of 2,461 identified CSF proteins were clustered using Mfuzz into 8 discrete clusters (Figure S8). Among them, proteins in cluster 7 and cluster 8 showed the same regulatory trend with disease progression (Figure 5A). The levels of 18 selected significantly dysregulated proteins (ANOVA $p < 0.05$ in cluster 7, ANOVA $p < 0.01$ in cluster 8) are shown in the heatmap in Figure 5B. Network pathway analysis of the dysregulated proteins revealed several important molecular-related pathways, including pathways involving insulin, prolactin, calcium-dependent protein kinase II, microtubule-associated protein tau (MAPT), and others, as shown in Figure S9. Several previously recognized AD CSF biomarkers,[20] including GFAP, MAPT, NEFL, and neurogranin (NRGN), were among them; the levels of these biomarkers are shown by the boxplots in Figure 5C.

To identify blood-based AD staging biomarkers, we compared the dysregulated proteins in serum samples along the trajectory of AD. A total of 1,330 identified proteins were clustered using Mfuzz into 8 discrete clusters (Figure S10). Among them, proteins in cluster 5 and cluster 6 showed the same regulatory trend with disease progression (Figure 5D). The levels of 18 selected significantly dysregulated proteins (ANOVA $p < 0.05$ in cluster 5 and cluster 6) demonstrating stage-dependent dysregulation are shown by the heatmap in Figure 5E. Several important proteins, including insulin, IGHM, PRDX2, and others, were identified by network pathway analysis, as shown in Figure S11.

Verification of proteins with AD stage–dependent dysregulation in the validation cohort

The validation cohort comprised 221 participants with CSF samples and 288 participants with serum samples. Regarding the CSF samples, a total of 21 core proteins with stage-dependent alterations were validated. The expression levels of 9 of them were downregulated with disease progression, whereas those of 12 of them were upregulated (Figure 6A). Remarkably, the expression level of ATRN was upregulated as the disease progressed. This protein has both membrane-bound and secreted protein isoforms (Figure 6B). ATRN has been reported to be differentially regulated in the blood samples of asymptomatic familial AD patients carrying *PSEN1* mutations.[21] In addition, 2 proteins, 14-3-3 protein epsilon (YWHAE) and 14-3-3 protein gamma (YWHAG), were upregulated over the disease progression (Figure 6B). CSF 14-3-3 proteins have already been used as surrogate markers of neuronal damage for AD, PD, and ALS but lack specificity.[22] Our results are consistent with several recent proteomic studies showing that YWHAE and YWHAG are promising AD staging biomarkers.[13,23]

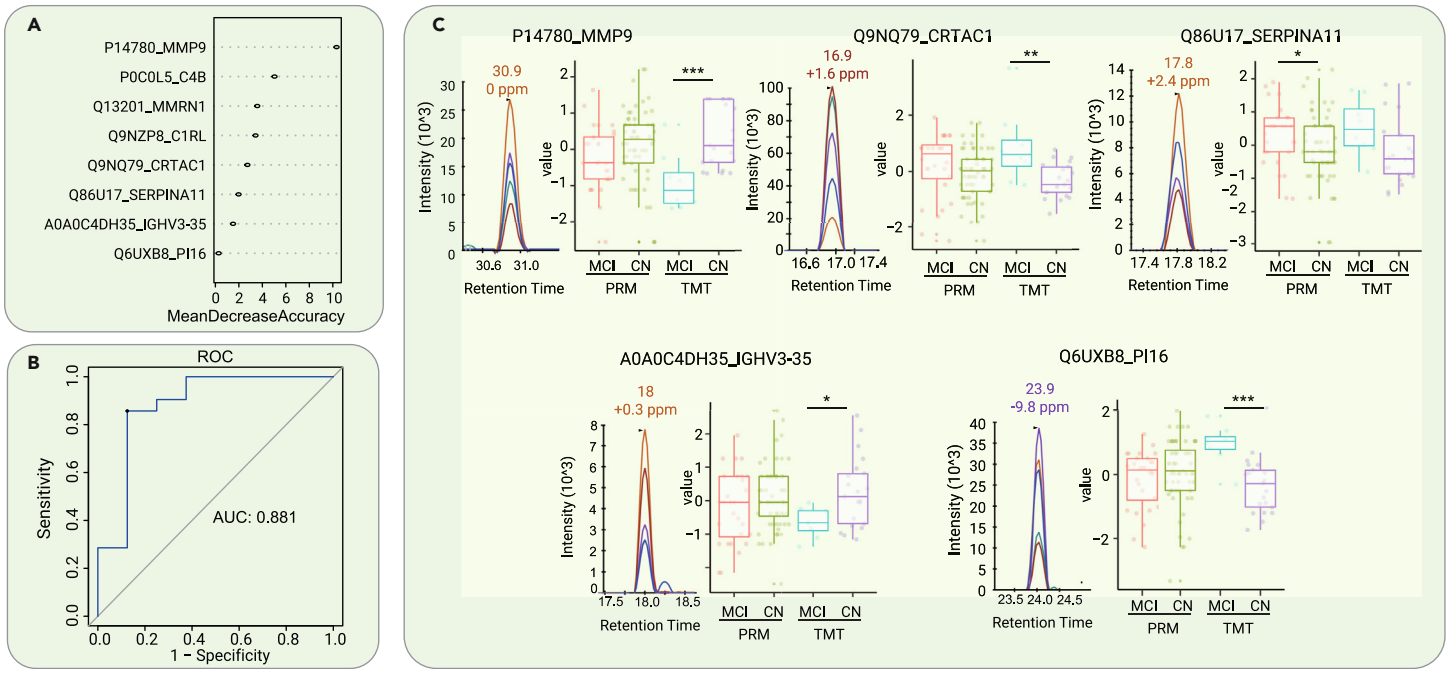

Figure 4. Differentiation of MCI due to AD and CN by machine learning of serum proteomic features (A) Top 8 proteins prioritized by random forest analysis ranked by the mean decrease in accuracy. (B) ROC curve of the random forest model. (C) Expression level change (*Z* scored original value) of the 5 core proteins with significant differences between patients with MCI due to AD and CN participants in both TMT-based and PRM proteomic analyses. *p < 0.05; **p < 0.01; ***p < 0.005.

Regarding the serum samples, a total of 18 core proteins exhibited stage-dependent alterations. The levels of 5 of them were downregulated, whereas those of 13 of them were upregulated with disease progression (Figure 6C). Notably, CFI was upregulated over the course of AD progression (Figure 6D). CFI is essential for regulating the complement cascade. Complement pathway hyperactivation has been found in an AD mouse model.[24] In addition, PRDX2 was found to be dysregulated in serum during the development of AD (Figure 6D). Interestingly, similar to the results found in CSF, another 14-3-3 protein, YWHAQ, was found to be dysregulated in serum in the different stages of AD (Figure 6D).

DISCUSSION

In this study, we performed one of the most in-depth proteomic analyses using paired CSF and serum samples acquired from AD patients. Our proteomic data mirrored a variety of disease-associated changes in the early stage and developmental trajectory of AD. Furthermore, based on an independent multicenter validation cohort, we developed a 19-protein CSF panel and an 8-protein serum panel for the early diagnosis of AD by machine learning. We used these panels to establish a highly accurate model for discriminating participants with MCI due to AD from CN participants. In addition, we verified 21 CSF and 18 serum core AD stage-dependent dysregulated proteins.

The leading dysregulated CSF and serum molecules during the early stage of AD are involved in IGF-1 signaling, ECM dysfunction, immune response pathways, lipid metabolism, Golgi and lysosome pathways, and oxidative species metabolism. Our CSF discovery dataset showed partial overlap with the results of several recent AD CSF proteomic studies.[13,23,25] Notably, one plasma proteomic study developed a 19-protein blood-based panel that could accurately distinguish AD patients from healthy controls (AUC = 0.9690–0.9816).[26] We narrowed the number of proteins to 8 in our serum-based panel that could accurately discriminate MCI due to AD from CN (AUC = 0.881), making it more convenient for clinical application in identifying MCI due to AD.

Our study revealed the differential activation of various biological pathways throughout the trajectory of AD, with the inflammatory pathway, synapse impairment pathway, and ECM dysfunction pathways emerging as key players. Neuroinflammation and related immune changes in the AD brain have been discussed intensely.[27] Our results identified several biomarkers involved in the inflammatory and immune response pathways that were significantly changed during the trajectory of the disease, including CXCL16, ATRN, CFI, and others. These findings, which are consistent with those from previous studies,[28] supported the growing evidence that neuroinflammation is an early event in AD and dynamically changes with disease development. It is well known that the levels of proteins associated with neuron or synapse degeneration pathways are increased in the CSF of AD patients.[29] Our data uncovered a series of known degeneration-related biomarkers (tau, NEFL, and NRGN), as well as several novel synapse-related biomarkers (YWHAE, YWHAG, YWHAQ, NRN1, NPTX2, and NPTXR).

In addition, our study found that the levels of proteins associated with ECM dysfunction, including COL15A1, PCOLCE, and PVR, were increased in the CSF and serum in AD. The role of ECM dysfunction in AD has attracted tremendous attention in recent years.[30] It is closely related to blood–brain barrier breakdown, which has been considered an early event of cognitive decline in AD patients.[31,32] These results are consistent with several recent proteomic studies performed in AD patients.[33,34]

The use of paired CSF and serum proteomics is more conducive to investigating the link between protein alterations in the central and peripheral environments in AD. Remarkably, proteins involved in the immune response–related, ECM-related, insulin-related, and synapse impairment pathways were significantly altered in both the CSF and serum of AD patients.

This study has several limitations. First, owing to the cross-sectional design of the study and the relatively small scale of the discovery cohort, further studies are necessary to confirm these results in a larger, longitudinal cohort. Second, the validation study used 4 specifically selected cohorts, and it would be better to validate the results in unselected longitudinal populations. Finally, in this study, only representative neurodegenerative diseases were selected as disease controls.

In conclusion, our study identified an 8-protein serum biomarker panel that has comparable power in identifying the early stage of AD to a 19-protein CSF biomarker panel. Moreover, we identified 21 CSF and 18 serum proteins reflecting different AD stages. Our findings provide a foundation for developing blood-based tests for clinical AD screening and staging.

MATERIALS AND METHODS

Participants

In the discovery cohort, 98 individuals with paired CSF and serum samples were recruited from the Second Affiliated Hospital of Zhejiang University School of Medicine between August 2015 and January 2021 (Tables S1 and S3A). The diagnoses of AD and MCI due to AD were based on the National Institute on Aging-Alzheimer's Association (NIA-AA) AT(N) criteria.[5] ALS patients were diagnosed according to the El Escorial criteria for ALS.[35] HD patients were diagnosed by the presence of typical clinical manifestations and a positive *HTT* gene genetic test.[36] FTD patients were diagnosed according to previous criteria.[37] Patients received neuropsychological assessments, including the Mini-Mental

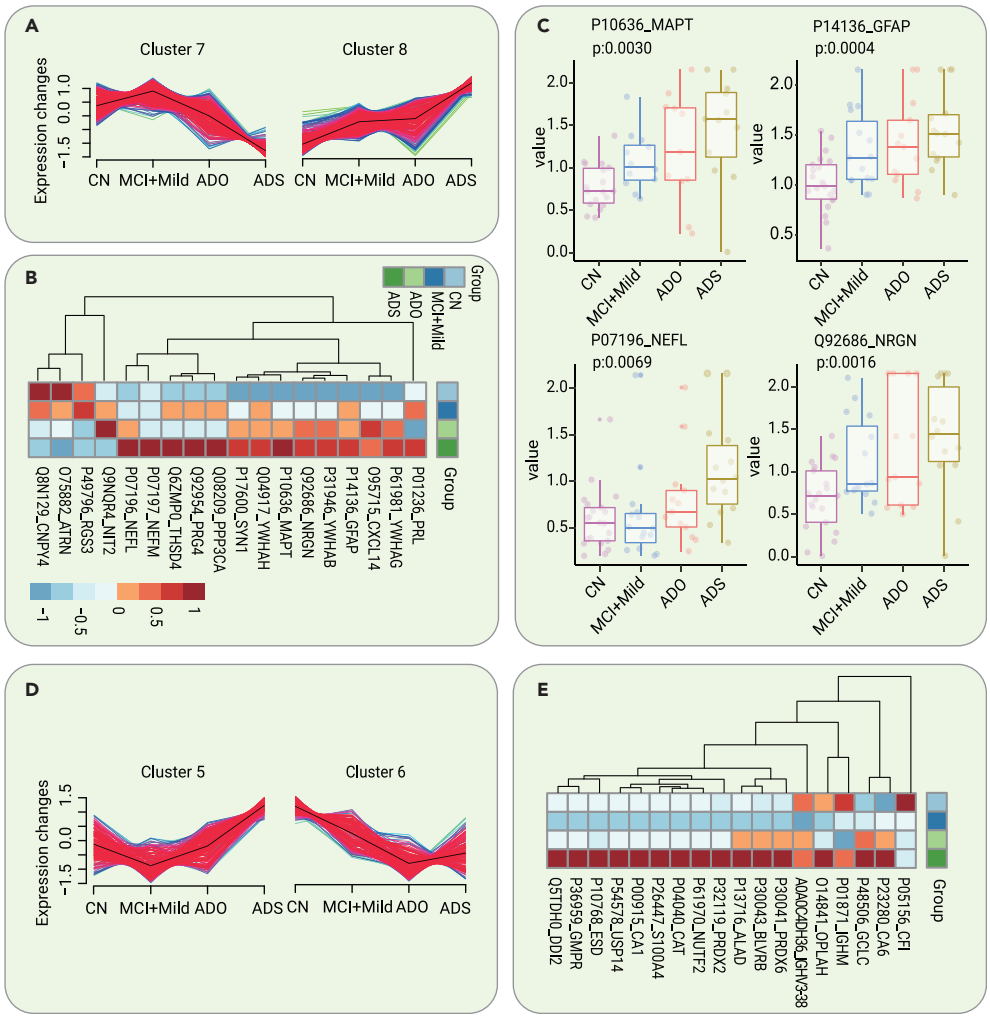

Figure 5. Dysregulated CSF and serum proteins as potential biomarkers for AD staging (A) Two clusters of CSF proteins identified with the Mfuzz analysis showed the same regulatory trend with disease progression. (B) Heatmap of the expression levels of the core dysregulated CSF proteins (ANOVA $p < 0.05$ in cluster 7, ANOVA $p < 0.01$ in cluster 8) in different stages of AD. (C) Expression level change (*Z* scored original value) of 4 recognized AD biomarkers with significant changes in the different stages of AD. (D) Two clusters of serum proteins identified with the Mfuzz analysis showed the same regulatory trend with disease progression. (E) Heatmap of the expression levels of the core dysregulated serum proteins (ANOVA $p < 0.05$) in different stages of AD.

State Examination, the Clinical Dementia Rating (CDR), and the Montreal Cognitive Assessment. Measurements of CSF biomarkers ($A\beta_{42}$, tau, and p-tau_{181}) or Pittsburgh compound B (PET/PIB) PET imaging were also conducted. The AD group was further classified into the ADM, ADMO, and ADS groups according to the CDR. The CN group comprised patients with other noncentral nervous system diseases without dementia and evidence of an underlying AD pathophysiologic process.

The participants in the validation cohort were recruited from Xuanwu Hospital affiliated with Capital Medical University, the First and Second Affiliated Hospitals of Zhejiang University School of Medicine, and the First Affiliated Hospital of Xiamen University. The validation cohort comprised 221 participants with CSF samples and 288 participants with serum samples (Tables S2 and S4A). The demographic data are presented in Tables S1 and S2.

ELISAs for measurement of CSF $A\beta_{42}$, t-tau, and p-tau_{181} levels

CSF $A\beta_{42}$, t-tau, and p-tau_{181} levels were measured by ELISA kits (Fujirebio, Ghent, Belgium) according to the manufacturer's instructions, as described in our previous study.[38]

Blood biomarker assessment

Serum GFAP and NEFL were quantified by commercially available Single Molecular Immunity Detection kits (Astrabio, R14060 and R14040). All of the measurements were conducted on an AST-Sc-Lite analyzer (Astrabio) and were performed according to the manufacturer's instructions.

Proteome analysis

Immunodepleting was implemented before digestion to increase the depth of the CSF and serum proteomes. Briefly, 100 and 175 μL of depletion resin (Thermo Scientific) were used for 100 μL of CSF and 4 μL of serum, respectively.

TMT-based proteomics analysis was performed as previously described.[12] The detailed procedures are described in the supplemental information.

Quality control of TMT-based proteome data

We divided the 98 samples into 7 batches according to disease type, age, and sex (Table S3A). We randomly selected one CSF and serum sample from each type of patient as a biological replicate to control the quality of the proteome discovery workflow. Our data exhibited a high degree of consistency and reproducibility, with median coefficients of variation (CVs) for 7 biological replicates below 0.16 (Figures S12A and S12B). Visualization of the data obtained from the pooled serum and CSF peptide samples showed minimal batch effects (Figures S12C and S12D).

Targeted proteomics analysis

Peptide samples were prepared in the same way as described in the previous proteomic section, except that no depletion or TMT labeling was performed. The detailed procedures are described in the supplemental information. A total of 120 peptides, including 15 common internal retention time (CiRT) peptides[39] (Table S4B), were included in the CSF PRM experiment, whereas 52 peptides, including 13 CiRT peptides, were included in the serum PRM experiment (Table S4D). CiRT peptides were used for the prediction of retention time to improve the confidence in target peptide identification.[40] The PRM data were manually analyzed with Skyline[41] and ProteomeExpert.[42]

Quality control of PRM proteome data

We selected 11 CSF samples and 16 serum samples as technical replicates, and the median CVs were below 0.15 (Figures S13A and S13B). We also prepared pooled CSF and serum peptide samples to evaluate the reproducibility of the PRM workflow. The Pearson correlation coefficient (r) of the proteomics data for 8 CSF pooled samples and 10 serum pooled samples was calculated, and all of the median r values were 0.99 (Figures S13C and S13D). We also observed fewer batch effects using the pooled samples (Figures S13E and S13F).

Statistical analysis and machine learning

For each pair of compared groups, the two-sided unpaired Welch's t test was conducted for statistical analysis. Pearson's r was calculated using the "cor" function in R (version 4.0.2) with the "pairwise.complete.obs" parameter to handle missing values. Machine learning was carried out using the R package randomForest (version 4.6.14), with some modifications based on previous work,[12] briefly described as follows. The key random forest parameters, including the mean decrease accuracy cutoff, number of iterations of cross-validation, and number of trees, were optimized. The input protein features were selected based on the mean decrease accuracy cutoff. Five-fold cross-validation was performed, and a total of 1,000 and 600 trees were built for the CSF model and the serum model, respectively. The minimum decreasing mean accuracy of protein features was set to 3 for the CSF model and 0 for serum features. The mtry values for the CSF and serum models were set to the square roots of 4 and 2, respectively.

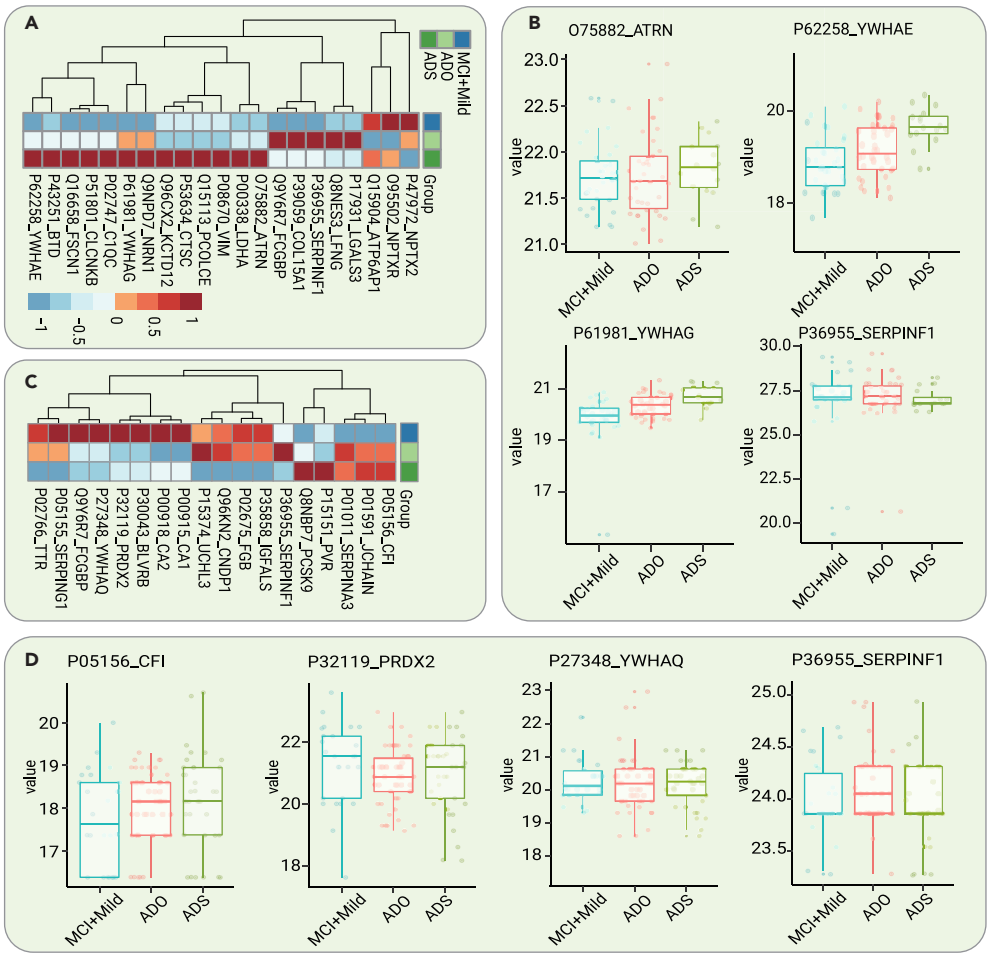

Figure 6. Verification of AD stage-dependent dysregulated proteins in the validation cohort (A) Heatmap of the levels of the validated core dysregulated CSF proteins in different stages of AD. (B) Expression level change (*Z* scored original value) of 4 selected CSF proteins dysregulated over the course of AD progression. (C) Heatmap of the levels of the validated core dysregulated serum proteins in different stages of AD. (D) Expression level change (*Z* scored original value) of 4 selected serum proteins dysregulated over the course of AD progression.

DATA AND CODE AVAILABILITY

The raw MS data in this study have been deposited to the ProteomeXchange Consortium (http://proteomecentral.proteomexchange.org) via the iProX partner repository with the dataset identifier PXD039146.

REFERENCES

1. Scheltens, P., De Strooper, B., Kivipelto, M., et al. (2021). Alzheimer's disease. Lancet ***397***, 1577–1590.
2. Wang, H., Dey, K.K., Chen, P.C., et al. (2020). Integrated analysis of ultra-deep proteomes in cortex, cerebrospinal fluid and serum reveals a mitochondrial signature in Alzheimer's disease. Mol. Neurodegener. ***15***, 43.
3. Palmqvist, S., Insel, P.S., Stomrud, E., et al. (2019). Cerebrospinal fluid and plasma biomarker trajectories with increasing amyloid deposition in Alzheimer's disease. EMBO Mol. Med. ***11***, e11170.
4. Panyard, D.J., McKetney, J., Deming, Y.K., et al. (2023). Large-scale proteome and metabolome analysis of CSF implicates altered glucose and carbon metabolism and succinylcarnitine in Alzheimer's disease. Alzheimers Dement.
5. Jack, C.R., Jr., Bennett, D.A., Blennow, K., et al. (2018). NIA-AA Research Framework: Toward a biological definition of Alzheimer's disease. Alzheimers Dement. ***14***, 535–562.
6. Dubois, B., Villain, N., Frisoni, G.B., et al. (2021). Clinical diagnosis of Alzheimer's disease: recommendations of the International Working Group. Lancet Neurol. ***20***, 484–496.
7. Teunissen, C.E., Verberk, I.M.W., Thijssen, E.H., et al. (2022). Blood-based biomarkers for Alzheimer's disease: towards clinical implementation. Lancet Neurol. ***21***, 66–77.
8. Oeckl, P., Anderl-Straub, S., Von Arnim, C.A.F., et al. (2022). Serum GFAP differentiates Alzheimer's disease from frontotemporal dementia and predicts MCI-to-dementia conversion. J. Neurol. Neurosurg. Psychiatry ***93***, 659–667.
9. Palmqvist, S., Janelidze, S., Quiroz, Y.T., et al. (2020). Discriminative Accuracy of Plasma Phospho-tau217 for Alzheimer Disease vs Other Neurodegenerative Disorders. JAMA ***324***, 772–781.
10. Egan, M.F., Kost, J., Voss, T., et al. (2019). Randomized Trial of Verubecestat for Prodromal Alzheimer's Disease. N. Engl. J. Med. ***380***, 1408–1420.
11. Long, J.M., and Holtzman, D.M. (2019). Alzheimer Disease: An Update on Pathobiology and Treatment Strategies. Cell ***179***, 312–339.
12. Shen, B., Yi, X., Sun, Y., et al. (2020). Proteomic and Metabolomic Characterization of COVID-19 Patient Sera. Cell ***182***, 59–72.e15.
13. Bai, B., Vanderwall, D., Li, Y., et al. (2021). Proteomic landscape of Alzheimer's Disease: novel insights into pathogenesis and biomarker discovery. Mol. Neurodegener. ***16***, 55.
14. Johnson, E.C.B., Dammer, E.B., Duong, D.M., et al. (2020). Large-scale proteomic analysis of Alzheimer's disease brain and cerebrospinal fluid reveals early changes in energy metabolism associated with microglia and astrocyte activation. Nat. Med. ***26***, 769–780.
15. Chen, M., and Xia, W. (2020). Proteomic Profiling of Plasma and Brain Tissue from Alzheimer's Disease Patients Reveals Candidate Network of Plasma Biomarkers. J. Alzheimers Dis. ***76***, 349–368.
16. Ehtewish, H., Mesleh, A., Ponirakis, G., et al. (2023). Blood-Based Proteomic Profiling Identifies Potential Biomarker Candidates and Pathogenic Pathways in Dementia. Int. J. Mol. Sci. ***24***, 8117.
17. Kumar, L., and E Futschik, M. (2007). Mfuzz: a software package for soft clustering of microarray data. Bioinformation ***2***, 5–7.
18. Liu, J., Huang, Y., Li, T., et al. (2021). The role of the Golgi apparatus in disease (Review). Int. J. Mol. Med. ***47***, 38.
19. Wang, H., Williams, D., Griffin, J., et al. (2017). Time-course global proteome analyses reveal an inverse correlation between Abeta burden and immunoglobulin M levels in the APPNL-F mouse model of Alzheimer disease. PLoS One ***12***, e0182844.
20. Leuzy, A., Cullen, N.C., Mattsson-Carlgren, N., et al. (2021). Current advances in plasma and cerebrospinal fluid biomarkers in Alzheimer's disease. Curr. Opin. Neurol. ***34***, 266–274.
21. Muenchhoff, J., Poljak, A., Thalamuthu, A., et al. (2016). Changes in the plasma proteome at asymptomatic and symptomatic stages of autosomal dominant Alzheimer's disease. Sci. Rep. ***6***, 29078.
22. Steinacker, P., Aitken, A., and Otto, M. (2011). 14-3-3 proteins in neurodegeneration. Semin. Cell Dev. Biol. ***22***, 696–704.
23. Bader, J.M., Geyer, P.E., Müller, J.B., et al. (2020). Proteome profiling in cerebrospinal fluid reveals novel biomarkers of Alzheimer's disease. Mol. Syst. Biol. ***16***, e9356.
24. Morgan, B.P. (2018). Complement in the pathogenesis of Alzheimer's disease. Semin. Immunopathol. ***40***, 113–124.
25. Whelan, C.D., Mattsson, N., Nagle, M.W., et al. (2019). Multiplex proteomics identifies novel CSF and plasma biomarkers of early Alzheimer's disease. Acta Neuropathol. Commun. ***7***, 169.
26. Jiang, Y., Zhou, X., Ip, F.C., et al. (2022). Large-scale plasma proteomic profiling identifies a high-performance biomarker panel for Alzheimer's disease screening and staging. Alzheimers Dement. ***18***, 88–102.

27. Kinney, J.W., Bemiller, S.M., Murtishaw, A.S., et al. (2018). Inflammation as a central mechanism in Alzheimer's disease. Alzheimers Dement. (N Y) ***4***, 575–590.
28. Ismail, R., Parbo, P., Madsen, L.S., et al. (2020). The relationships between neuroinflammation, beta-amyloid and tau deposition in Alzheimer's disease: a longitudinal PET study. J. Neuroinflammation ***17***, 151.
29. Ramachandran, A.K., Das, S., Joseph, A., et al. (2021). Neurodegenerative Pathways in Alzheimer's Disease: A Review. Curr. Neuropharmacol. ***19***, 679–692.
30. Sun, Y., Xu, S., Jiang, M., et al. (2021). Role of the Extracellular Matrix in Alzheimer's Disease. Front. Aging Neurosci. ***13***, 707466.
31. Montagne, A., Nation, D.A., Sagare, A.P., et al. (2020). APOE4 leads to blood-brain barrier dysfunction predicting cognitive decline. Nature ***581***, 71–76.
32. Nation, D.A., Sweeney, M.D., Montagne, A., et al. (2019). Blood-brain barrier breakdown is an early biomarker of human cognitive dysfunction. Nat. Med. ***25***, 270–276.
33. Bai, B., Wang, X., Li, Y., et al. (2020). Deep Multilayer Brain Proteomics Identifies Molecular Networks in Alzheimer's Disease Progression. Neuron ***106***, 700.
34. Higginbotham, L., Ping, L., Dammer, E.B., et al. (2020). Integrated proteomics reveals brain-based cerebrospinal fluid biomarkers in asymptomatic and symptomatic Alzheimer's disease. Sci. Adv. ***6***, eaaz9360.
35. Brooks, B.R., Miller, R.G., Swash, M., et al. (2000). El Escorial revisited: revised criteria for the diagnosis of amyotrophic lateral sclerosis. Amyotroph. Lateral Scler. Other Motor Neuron Disord. ***1***, 293–299.
36. Li, H.L., Li, X.Y., Dong, Y., et al. (2019). Clinical and Genetic Profiles in Chinese Patients with Huntington's Disease: A Ten-year Multicenter Study in China. Aging Dis. ***10***, 1003–1011.
37. Boeve, B.F., Boxer, A.L., Kumfor, F., et al. (2022). Advances and controversies in frontotemporal dementia: diagnosis, biomarkers, and therapeutic considerations. Lancet Neurol. ***21***, 258–272.
38. Ye, L.Q., Gao, P.R., Zhang, Y.B., et al. (2021). Application of Cerebrospinal Fluid AT(N) Framework on the Diagnosis of AD and Related Cognitive Disorders in Chinese Han Population. Clin. Interv. Aging ***16***, 311–323.
39. Parker, S.J., Rost, H., Rosenberger, G., et al. (2015). Identification of a Set of Conserved Eukaryotic Internal Retention Time Standards for Data-independent Acquisition Mass Spectrometry. Mol. Cell. Proteomics ***14***, 2800–2813.
40. Zhu, T., Zhu, Y., Xuan, Y., et al. (2020). DPHL: A DIA Pan-human Protein Mass Spectrometry Library for Robust Biomarker Discovery. Dev. Reprod. Biol. ***18***, 104–119.
41. MacLean, B., Tomazela, D.M., Shulman, N., et al. (2010). Skyline: an open source document editor for creating and analyzing targeted proteomics experiments. Bioinformatics ***26***, 966–968.
42. Zhu, T., Chen, H., Yan, X., et al. (2021). ProteomeExpert: a Docker image-based web server for exploring, modeling, visualizing and mining quantitative proteomic datasets. Bioinformatics ***37***, 273–275.

ACKNOWLEDGMENTS

This work was supported by grants from the Key Research and Development project of Zhejiang Province (2019C03039), the National Natural Science Foundation of China (81970998), the Science Innovation 2030-Brain Science and Brain-Inspired Intelligence Technology Major Projects (nos. 2021ZD0201103 and 2021ZD0201803), and the Integrative Traditional Chinese and Western Medicine Innovation Team for Neurodegenerative Diseases of Zhejiang Province.

AUTHOR CONTRIBUTIONS

Conception and design, Q.-Q.T., X.C., T.G., and Z.-Y.W.; clinical sample/data collection, Q.-Q.T., Y.-Y.X., X.-Y.L., R.-R.L., G.-P.P., K.-M.Z., B.J., J.-P.J., and Z.-Y.W.; development of methodology, Q.-Q.T., X.C., W.G., Y.-Y.X., L.Y., W.J., and S.L.; data management and statistical analyses, W.G.; manuscript drafting, Q.-Q.T. and X.C.; study supervision, T.G. and Z.-Y.W.

DECLARATION OF INTERESTS

The authors declare no competing interests.

SUPPLEMENTAL INFORMATION

It can be found online at https://doi.org/10.1016/j.xinn.2023.100544.

LEAD CONTACT WEBSITE

https://person.zju.edu.cn/wuzhiying/.

The Innovation, Volume *5*

Supplemental Information

Alzheimer's disease early diagnostic and staging biomarkers revealed by large-scale cerebrospinal fluid and serum proteomic profiling

Qing-Qing Tao, Xue Cai, Yan-Yan Xue, Weigang Ge, Liang Yue, Xiao-Yan Li, Rong-Rong Lin, Guo-Ping Peng, Wenhao Jiang, Sainan Li, Kun-Mu Zheng, Bin Jiang, Jian-Ping Jia, Tiannan Guo, and Zhi-Ying Wu

Supplemental materials

Detailed methods

Enzyme-linked immunosorbent assays (ELISAs) for measurement of CSF Aβ42, t-tau, and p-tau181 levels

CSF Aβ42, T-tau, and p-tau181 levels were measured by ELISA Kits (Fujirebio, Ghent, Belgium) according to the manufacturer's instructions as described by our previous study.[1] Briefly, CSF samples, calibrators (CALs), Run Validation Controls (RVC) and all other reagents were thawed and allowed to reach room temperature before use. At the beginning of the tests, conjugate working solution 1 (75μL for Aβ42 and t-tau, and 25μL for p-tau181) and CSF sample/CAL/RVC (25μL for Aβ42 and t-tau, and 75μL for p-tau181) were added to the wells of the antibody-coated plate, and adequately mixed by carefully tapping the stripholder. After incubating in an incubator (60 minutes at 25°C for Aβ42, 16h at 25°C for t-tau, 16h at 4°C for p-tau), all strips were washed 5 times. Add 100μL Conjugate working solution 2 to each well, and incubate in an incubator at 25°C (30 minutes for Aβ42 and t-tau, 60 minutes for p-tau). After washing each well 5 times, add 100μL substrate working solution and incubate for 30 minutes at 25°C in the dark. To stop the reaction, add 50μL Stop Solution to each well and tap the stripholder carefully to ensure optimal mixing. Read the absorbance at 450 nm and calculate the concentration of Aβ42, t-tau and p-tau181.

Blood biomarkers assessment

Serum GFAP and NEFL were quantified by commercial-available Single Molecular Immunity Detection kits (Astrabio, R14060 and R14040). All measurements were performed on the AST-Sc-Lite analyzer (Astrabio) and according to the manufacturer's instructions. Briefly, 25 μL of serum sample was added to an incubation tube, followed by the addition of 25 μL of Reagent 1 which contained 0.1 mg/mL of magnetic beads coated with capture antibodies for GFAP and NEFL. The mixture was then mixed rapidly and incubated at 40°C for 6 minutes. Afterward, Reagent 2, containing detection antibodies labeled with single-molecule imaging fluorophores, was added and mixed, and the mixture was incubated at 40°C for 4 minutes. Subsequently, the reaction mixture was transferred to a flow-cell with a 2*2 mm (width*height) channel for magnetic beads manipulation and imaging. The magnetic beads in the mixture were then absorbed onto the surface of the channel in the flow-cell with the assistance of a permanent magnet. The unlabeled fluorophores were then eliminated by a gentle washing flow of wash buffer and fluorescent images were taken with an integrated fluorescent microscope. The single-molecule signals were analyzed by the machine and protein concentrations were calculated with a standard curve prepared in advance.

Untargeted proteome analysis

Immunodepleting was implemented before digestion to increase the depth of the CSF and serum proteomes. Briefly, 100 μL and 175 μL depletion resin (Thermo Scientific, A36372) were mixed with 100 μL CSF (1:1 CSF/resin volume ratio) and 4 μL serum (4:175 serum/resin volume ratio), respectively, and incubated at room temperature (RT) for 20 min. The mixture was centrifuged at 1000 × g for 2 min to collect the flow-through, which was concentrated by centrifugation at 12000

× g for 30 min in 3k MWCO columns with a molecular weight cutoff (MWCO) of 3 kDa (Thermo Scientific, Cat # 88512). We then added 6 M urea/2 M thiourea (Sigma-Aldrich, Cat # T8656-500G) to the same columns to exchange the buffer system for protein denaturation, and centrifuged at 12000 g until <50 µL solution remained in the chambers. The protein concentrations of depleted CSF and serum samples were determined by a bicinchoninic acid Protein Assay Kit (BCA, Sigma-Aldrich, BCA1 AND B9643) according to the manufacturer's instructions. Concentrated depleted samples were then reduced by 10 mM tris-2(-carboxyethyl)-phosphine (TCEP, Adamas-beta, Cat # 61820E) for 40 min at 32 °C, followed by alkylation with 40 mM Iodoacetamide (IAA, Sigma-Aldrich, Cat # I6125) for 40 min at RT in the dark. The solution of 6 M urea/2 M thiourea, TCEP and IAA were prepared with 100 mM TEAB to make sure the reaction system at a pH of 8.5. Then, we diluted the system with 150 µL 100mM TEAB to make the final concentration of urea/thiourea below 1.5M/0.5M for LysC digestion with 2.5 µg LysC (Hualishi Tech, Cat # HLS LYS002C) for 4 h in 1st step of digestion. Then, we further diluted the reaction system with 50 µL 100mM TEAB and added 2.5 µg trypsin (Hualishi Tech, Cat # HLS TRY001C) for 12 h in 2nd step of digestion. Similarly, serum samples were digested with 0.5 µg LysC and 0.625 µg trypsin in the same way as CSF samples. After being acidified with trifluoroacetic acid (TFA, Thermo Fisher Scientific, Cat # 85183) at a 1% final concentration, peptides were then desalted using 2 mg Solaµ HRP columns (Thermo Scientific, Cat # 60209-001) and the eluate was dried using a SpeedVac.

We performed the batch design to equally deposit samples obtained from individuals with different diseases in the same batch for CSF and serum in parallel. In this way, we designed seven batches, and each batch contained 15 samples and one pooled sample. For serum samples, 7 µg of peptide from each sample was labeled with 56 µg of Tandem mass tags (TMT) 16plex reagent (Thermo Fisher Scientific™, San Jose, USA, Cat # A44520) according to the manufacturer's instructions. Due to the lower peptide yield of CSF, 5 µg peptide from each CSF sample was labeled with 40 µg TMT16plex reagent. After 1 h of incubation at RT, the TMT labeling reaction was quenched by hydroxylamine. We utilized TMT16plex-126 to label a pooled serum peptide sample of 49 µg and a pooled CSF peptide sample of 35 µg, which were both produced by mixing equal amounts of peptide from all the serum or CSF samples, followed by equal division into seven batches after labeling quenching, respectively. In this way, 15 labeled samples in the same batch and a labeled pool were combined and desalted using C18 columns (Waters, Sep-Pak Vac tC18 1cc, 50 mg, WAT054960). Fractionation was performed on a Thermo µLtimate Dinex 3000 (Thermo Fisher Scientific™, San Jose, USA) equipped with an XBridge Peptide BEH C18 column (300A, 5 µm × 4.6 mm × 250 mm) (Waters, Milford, MA, USA). Batches were separated using a 60 min gradient from 5% to 35% acetonitrile (ACN) in 10 mM ammonia (pH=10.0) at a flow rate of 1 mL/min to 60 fractions. We further combined the fractions of equal distance (1st and 31st, 2nd and 32nd, …,30th and 60th) to 30 fractions and used speedvac to dry the samples.

Dried peptide powder was re-dissolved in 2% ACN/0.1% formic acid (FA, Thermo Fisher Scientific, Cat # A117-50). Peptide samples were centrifuged at 15000 g for 15 min and then the

supernatants were transferred to sample vials, followed by analysis on LC-MS/MS. The MS raw data were searched by Proteome Discoverer (Version 2.4.1.15, Thermo Fisher Scientific) against a fasta file of Human proteins downloaded from https://www.uniprot.org/ on 7th May 2020, containing 20377 reviewed entries. Precursor ion mass tolerance was set to 10 ppm, and product ion mass tolerance was set to 0.02 Da. Other parameters are kept as default, including the FDR of 1% for PSM level, peptide level and protein level. The target-decoy strategy was setting Automatic, and the software checks whether all searches were validated in same mode in the processing step. The Grouped abundance ratio of 15 samples to pooled sample in the same batch was selected as the intensity of proteins in the protein matrix for the following statistical analysis.

Quality control of TMT-based proteome data

We randomly selected one CSF sample and one serum sample from each type of patient as a biological replicate, and randomly distributed these seven biological replicates into seven batches to control the quality of the proteome discovery workflow. Our data performed a high degree of consistency and reproducibility with the median coefficients of variations (CVs) for 7 biological replicates all below 0.16 (**Figure S11A, B**). Visualization of pooled serum and CSF peptide samples showed minimal batch effects (**Figure S11C, D**).

Targeted proteome analysis

Peptide samples were prepared in the same way as described in the previous proteomic section except that no depletion or TMT labeling was performed. A nanoflow DIONEX UltiMate 3000 RSLCnano System (Thermo Fisher Scientific™, San Jose, USA) coupled with a Q Exactive HF hybrid Quadrupole-Orbitrap (Thermo Fisher Scientific™, San Jose, USA) was applied for the parallel reaction monitoring (PRM) experiment. For each PRM acquisition, 0.5 μg of peptides was injected. The CSF peptide digests were separated at a flow rate of 300 nL/min (precolumn, 3 μm, 100 Å, 20 mm*75 μm internal diameter; analytical column, 1.9 μm, 120 Å, 150 mm*75 μm internal diameter.) with a 60 min effective gradient (from 10% to 30% buffer B). Buffer A was HPLC-grade water containing 2% ACN and 0.1% FA, and buffer B was 98% ACN containing 0.1% FA. The serum peptide digests were separated with 30 min effective gradient (from 10% to 30% buffer B). The resolution values for the full MS and PRM were 60,000 (at *m/z* 200) and 30,000 (at *m/z* 200), respectively. The automatic gain control (AGC) target was set to 2e5, and the maximum IT was set to 80 ms for PRM setting.

The PRM data were manually analyzed with Skyline.[2] The retention time was predicted by the common internal retention time (CiRT) peptides,[3] and the isolation time window was set to 5 min. The mass analyzer for MS1 and MS/MS was set to "Orbitrap", with a resolution power value of 60,000 and 30,000, respectively. We selected the top 6 peptides in terms of abundance for each target protein for detection. Based on the preliminary screening results, we selected 1-2 peptides for final detection for each protein. The final peptides should meet the following empirical criteria mentioned in the previous literature: [4,5] 1) accurate mass (mass error for precursors < 10 ppm, for fragments < 20 ppm), 2) good peak shape of the peak groups, 3) high abundance, 4) retention time within the

predicted range, 5) matching conditions for the abundance ratio of fragment ions with the library. Proteins that do not contain peptides that meet the above conditions are excluded. After selection, a total of 120 peptides including 15 CiRT peptides (**Table S3**) were included in the CSF PRM experiment while 52 peptides including 13 CiRT peptides (**Table S3**) were included in the serum PRM experiment. The value of total area fragment was exported as peptide relative quantitative data, and then converted to protein quantitative data using ProteomeExpert.[6]

REFERENCES

1. Ye, L.Q., Gao, P.R., Zhang, Y.B., et al. (2021). Application of Cerebrospinal Fluid AT(N) Framework on the Diagnosis of AD and Related Cognitive Disorders in Chinese Han Population. Clinical interventions in aging ***16***, 311-323, 10.2147/CIA.S294756.
2. MacLean, B., Tomazela, D.M., Shulman, N., et al. (2010). Skyline: an open source document editor for creating and analyzing targeted proteomics experiments. Bioinformatics ***26***, 966-968, 10.1093/bioinformatics/btq054.
3. Parker, S.J., Rost, H., Rosenberger, G., et al. (2015). Identification of a Set of Conserved Eukaryotic Internal Retention Time Standards for Data-independent Acquisition Mass Spectrometry. Molecular & cellular proteomics : MCP ***14***, 2800-2813, 10.1074/mcp.O114.042267.
4. Picotti, P., and Aebersold, R. (2012). Selected reaction monitoring-based proteomics: workflows, potential, pitfalls and future directions. Nature methods ***9***, 555-566, 10.1038/nmeth.2015.
5. Lange, V., Picotti, P., Domon, B., and Aebersold, R. (2008). Selected reaction monitoring for quantitative proteomics: a tutorial. Molecular systems biology ***4***, 222, 10.1038/msb.2008.61.
6. Zhu, T., Chen, H., Yan, X., et al. (2021). ProteomeExpert: a Docker image-based web server for exploring, modeling, visualizing and mining quantitative proteomic datasets. Bioinformatics ***37***, 273-275, 10.1093/bioinformatics/btaa1088.

Figure S1. Heatmap of the 3238 CSF proteins quantified by TMT-based LC-MS/MS analysis in the discovery cohort.

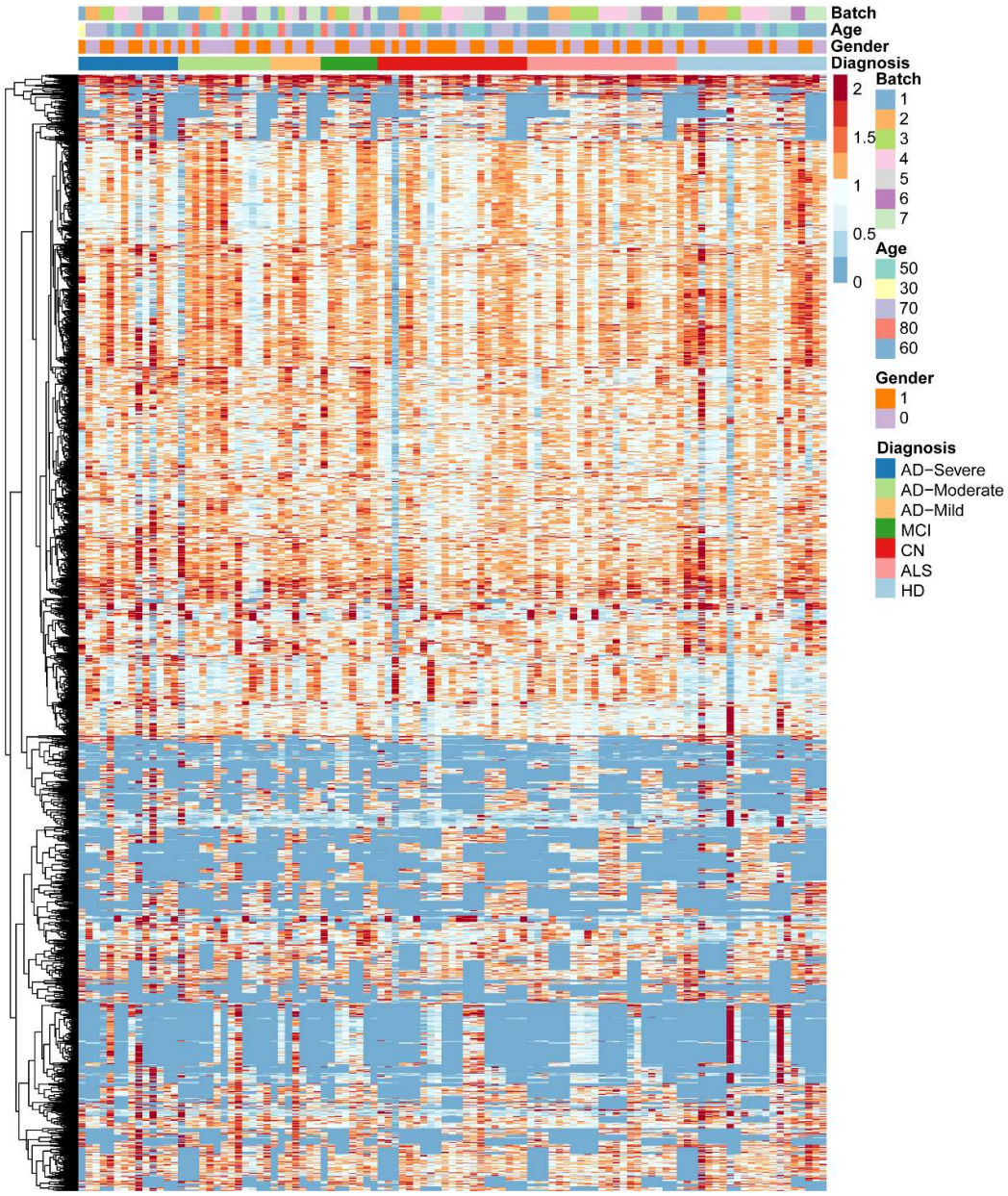

Figure S2. Heatmap of the 1702 quantified serum proteins by TMT-based LC-MS/MS analysis in the discovery cohort.

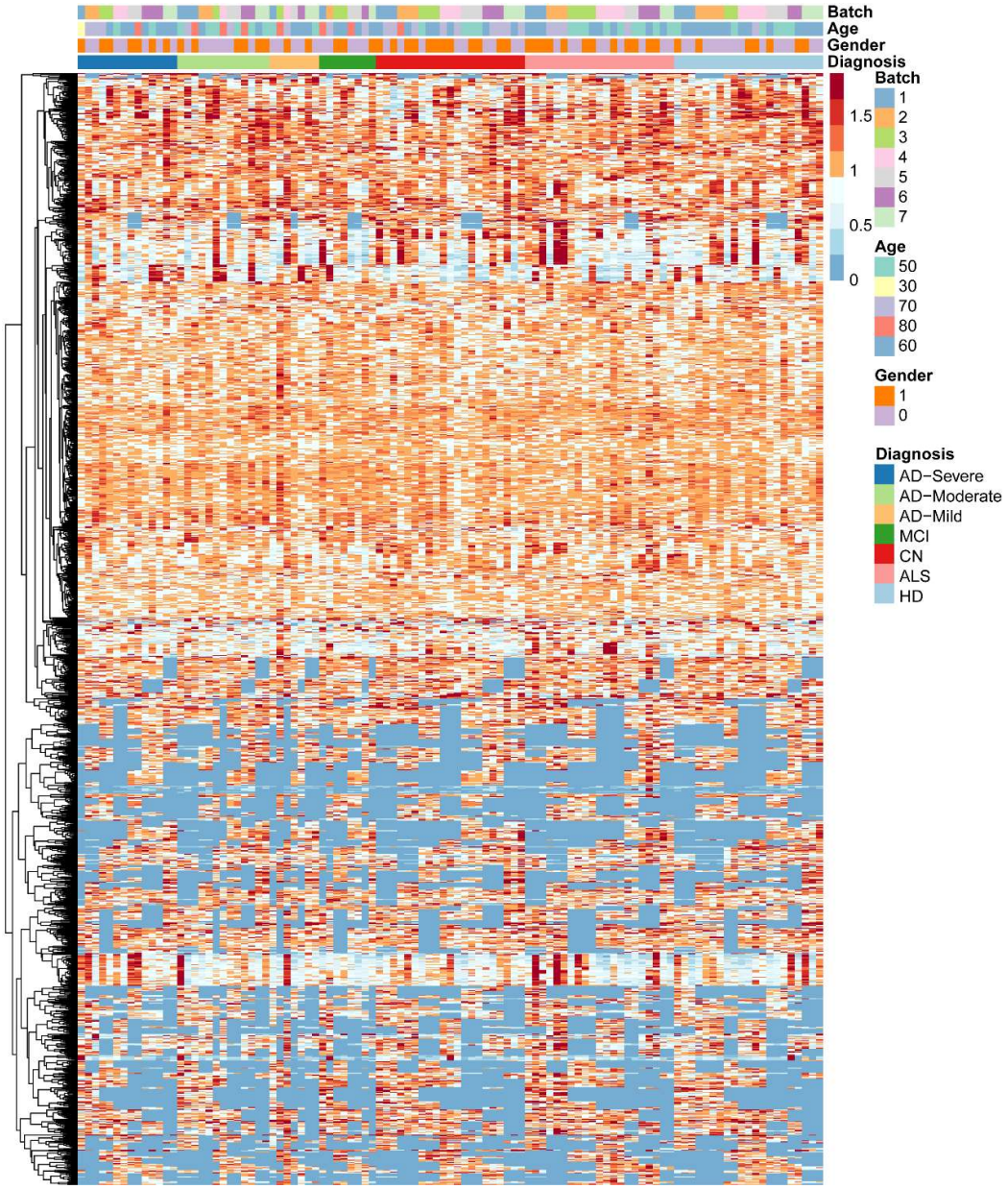

Figure S3. The ranking diagrams of CSF and serum proteins. **(A)** The average intensity of the 3238 CSF proteins identified by TMT-based proteomics was plotted with rank. All identified CSF proteins in this study are in blue for reference. The 19 CSF proteins selected by machine learning model were highlighted in red. **(B)** Concentration range of blood proteins. All identified serum proteins in this study are in blue for reference. The 8 serum proteins selected by machine learning model were highlighted in red.

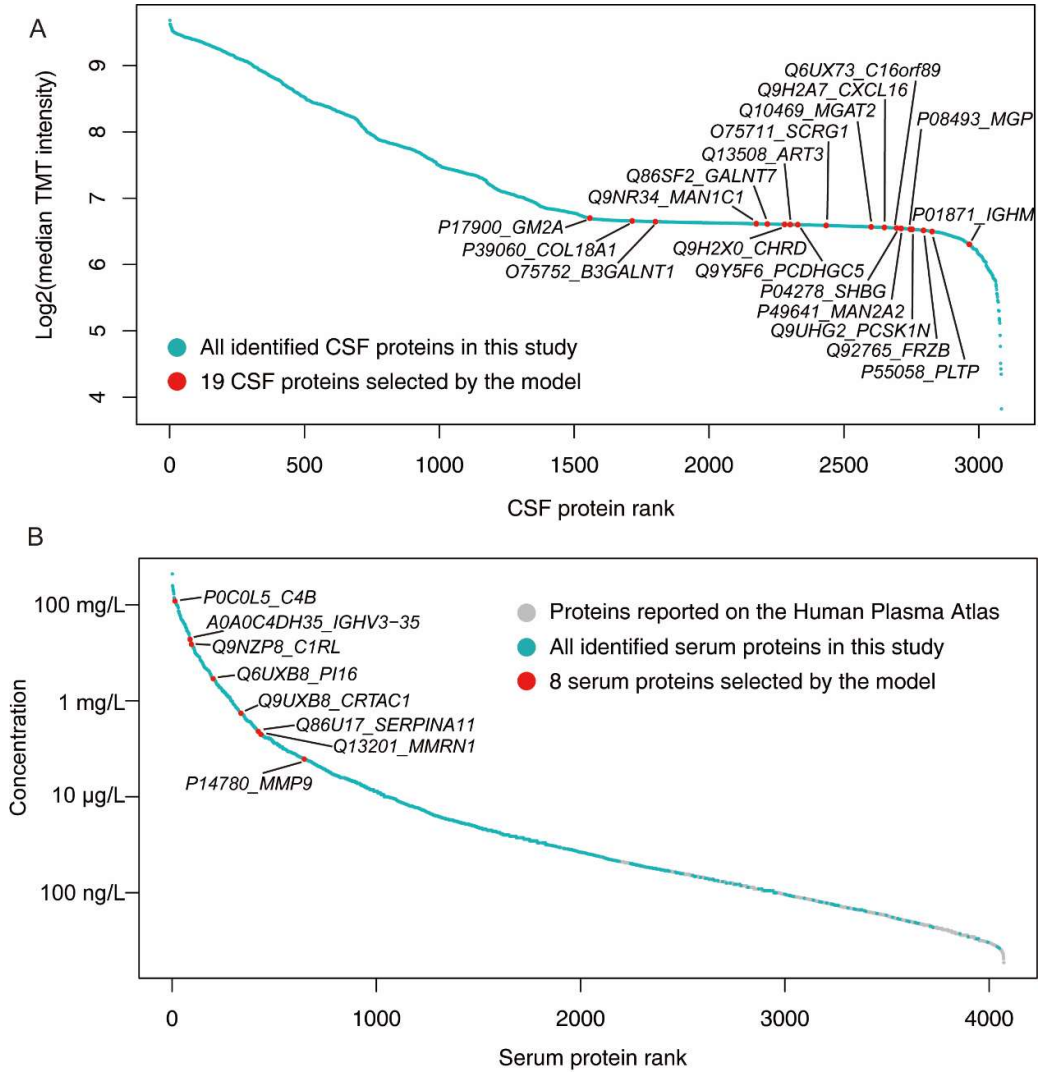

Figure S4. Validated selected differentially expressed proteins by real-time PCR. The transcription levels of the selected differentially expressed proteins (GFAP and GM2A) were evaluated by real-time PCR using the cortex of 5xFAD mice. The transcription levels of GFAP and GM2A were elevated in FAD as compared to wild type (WT) mice, which coincided with the results identified by TMT-based LC-MS/MS analysis. p-value: *, < 0.05; **, < 0.01; ***, < 0.005.

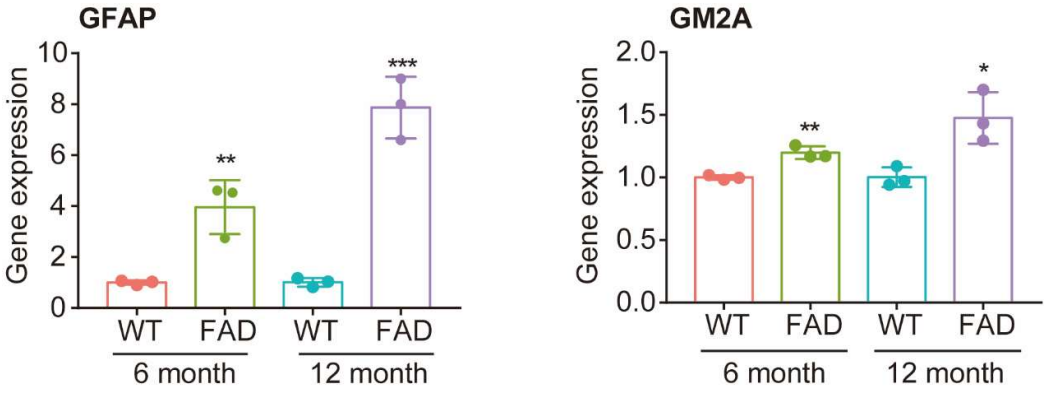

Figure S5. Evaluation of the protein biomarker panels to discriminate other neurodegenerative diseases by uniform manifold approximation and projection (UMAP). **(A)** The 19-protein CSF biomarker panel could well discriminate the MCI from FTD, ALS and HD patients. **(B)** The ability to discriminate the MCI from FTD, ALS and HD was relatively low by the 8-protein serum biomarker panel.

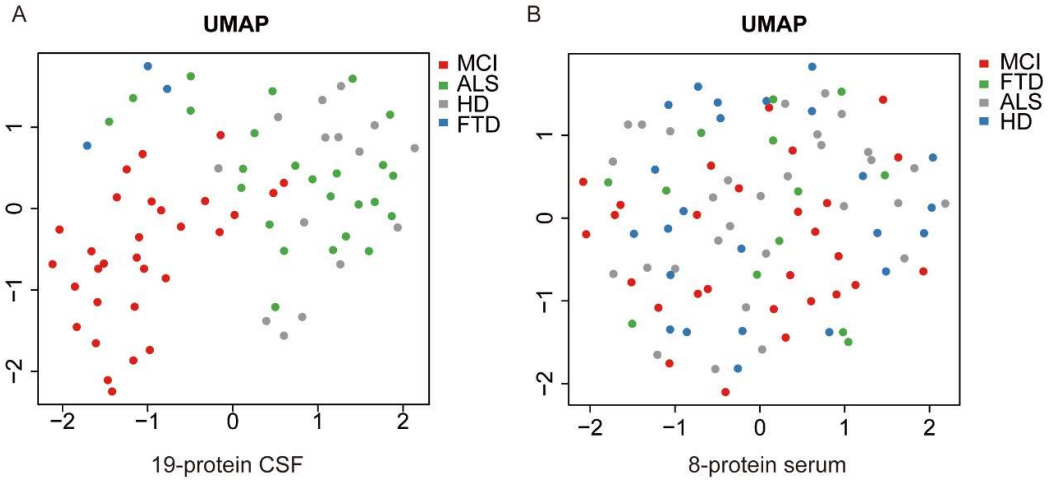

Figure S6. Evaluation of serum GFAP and NEFL to discriminate MCI due to AD and other neurodegenerative disease. (A) The expression level change of serum GFAP and NEFL detected by Single Molecular Immunity Detection kits in the CN controls, MCI due to AD, ALS and FTD. **(B)** Receiver operating characteristic (ROC) analysis was utilized to evaluate the efficacy of serum GFAP and NEFL in distinguishing between MCI due to AD and CN controls. **(C)** Evaluation of the serum GFAP and NEFL to discriminate other neurodegenerative diseases by uniform manifold approximation and projection (UMAP).

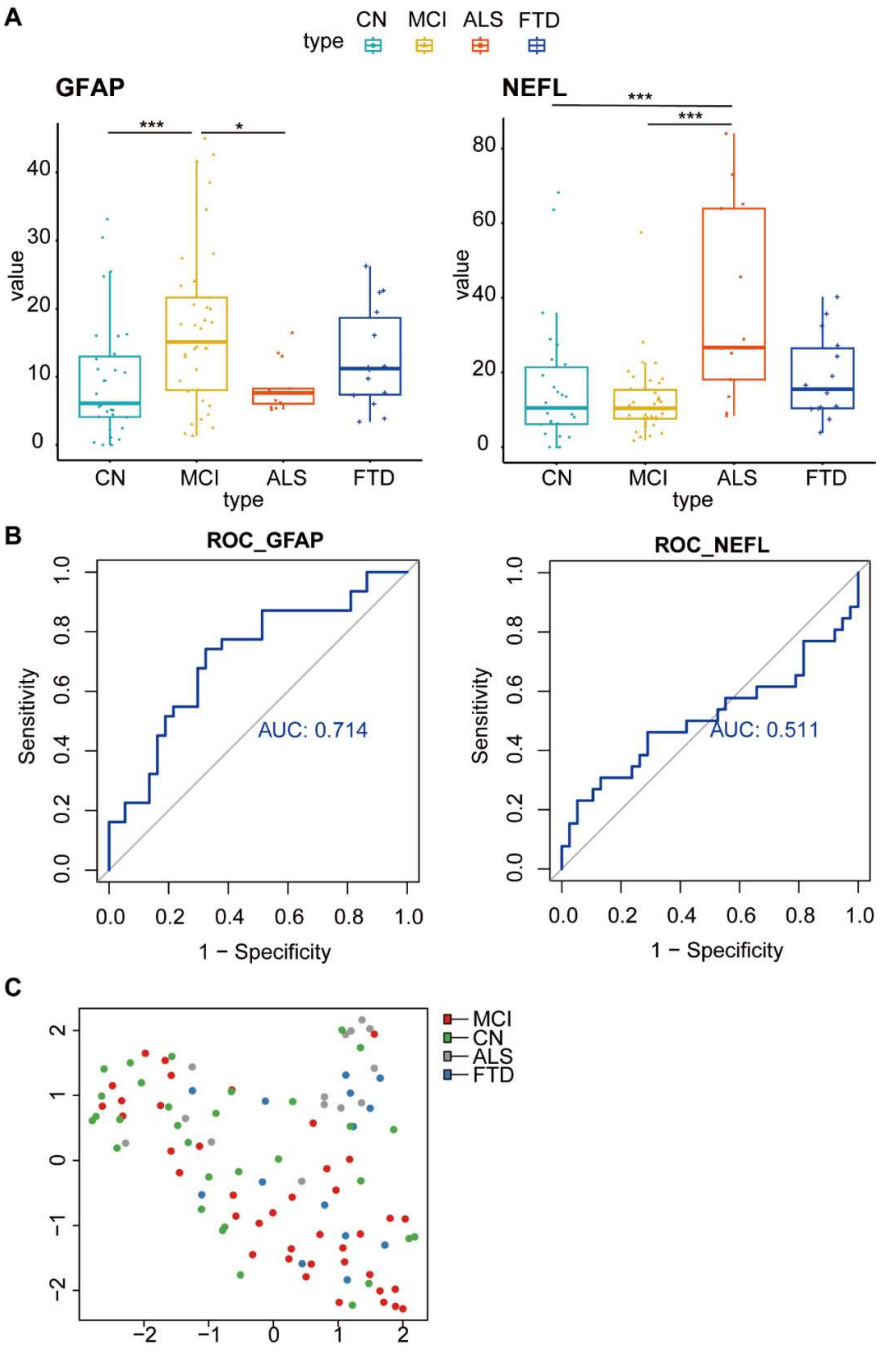

Figure S7. Correlations of the levels of CSF and serum core dysregulated proteins in MCI with the levels of CSF $A\beta_{42}$, t-tau and p-tau_{181}.

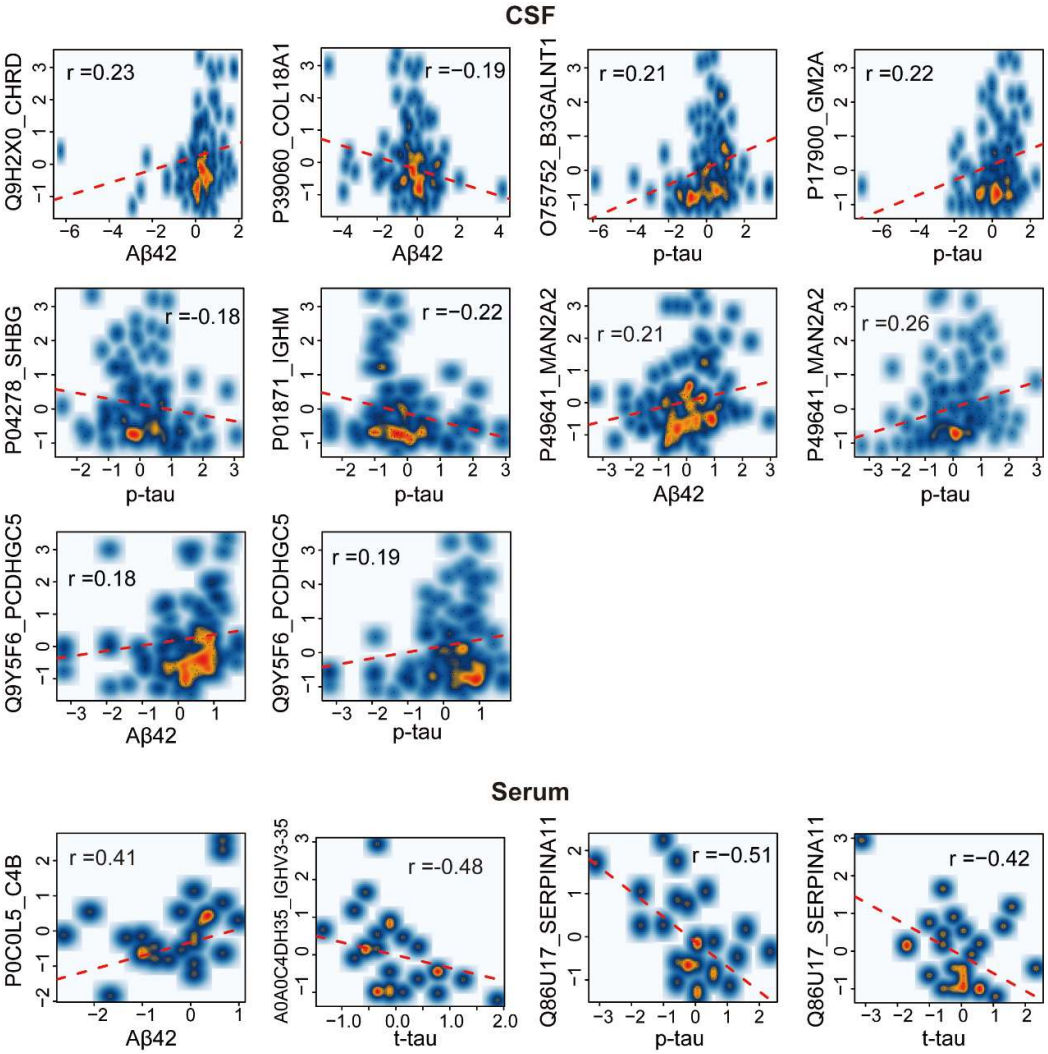

Figure S8. Eight clusters of 2461 CSF proteins identified with the Mfuzz analysis. Among them, proteins in cluster 7 and cluster 8 showed the same regulatory trend with disease progression.

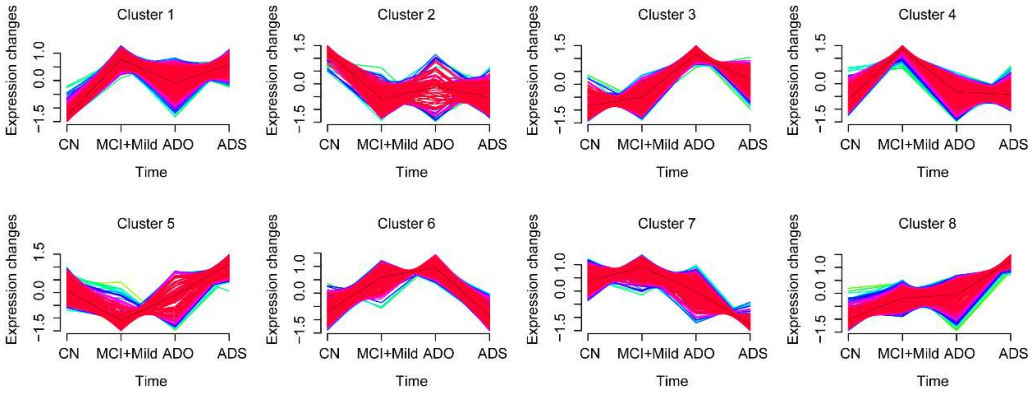

Figure S9. Network pathway analysis of dysregulated CSF proteins during the different stages of AD reveals several important molecular pathways.

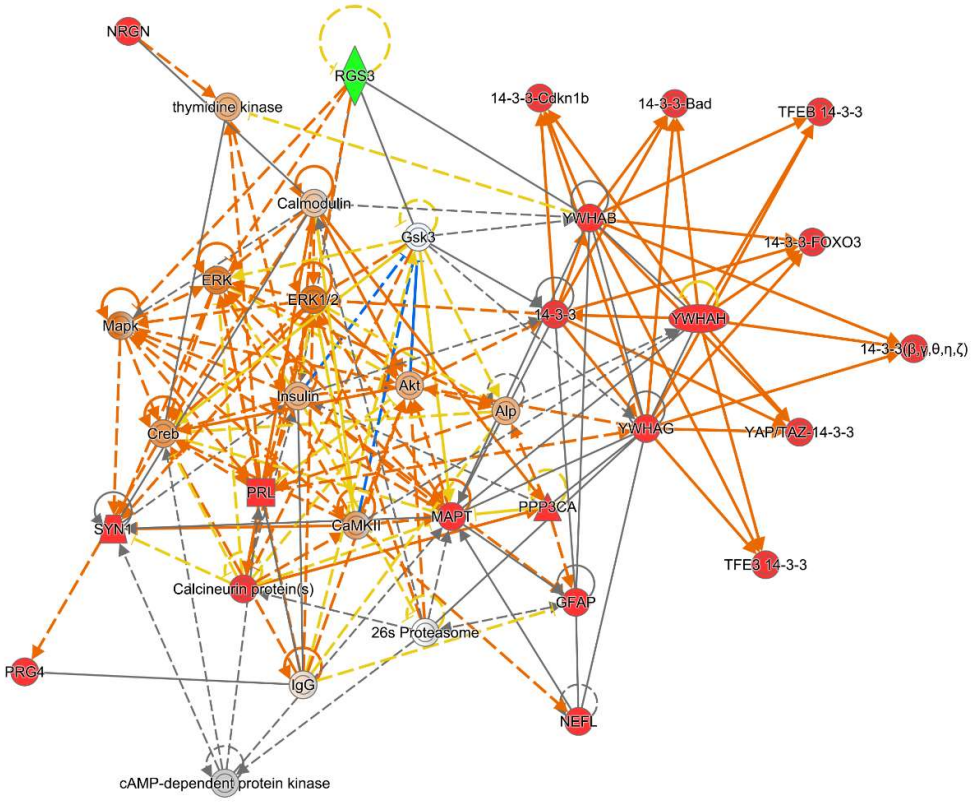

Figure S10. Eight clusters of 1330 serum proteins identified with the Mfuzz analysis. Among them, proteins in cluster 5 and cluster 6 showed the same regulatory trend with disease progression.

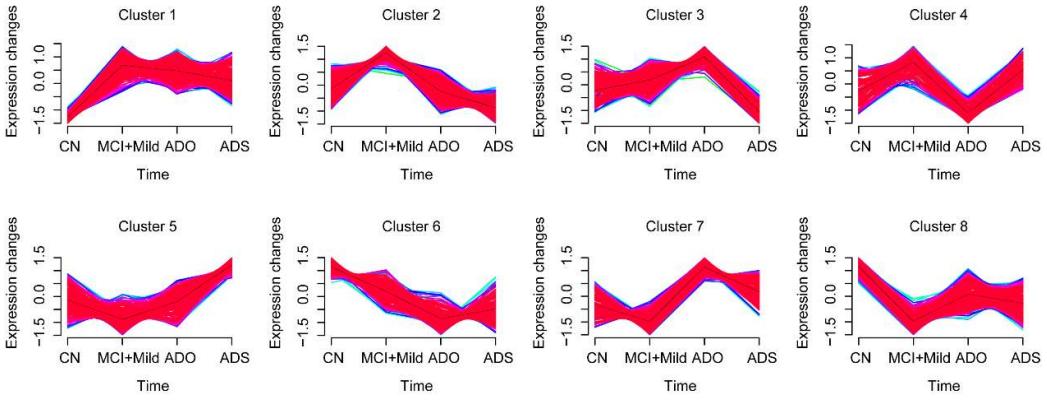

Figure S11. Network pathway analysis of dysregulated serum proteins during the different stages of AD reveals several important molecular pathways.

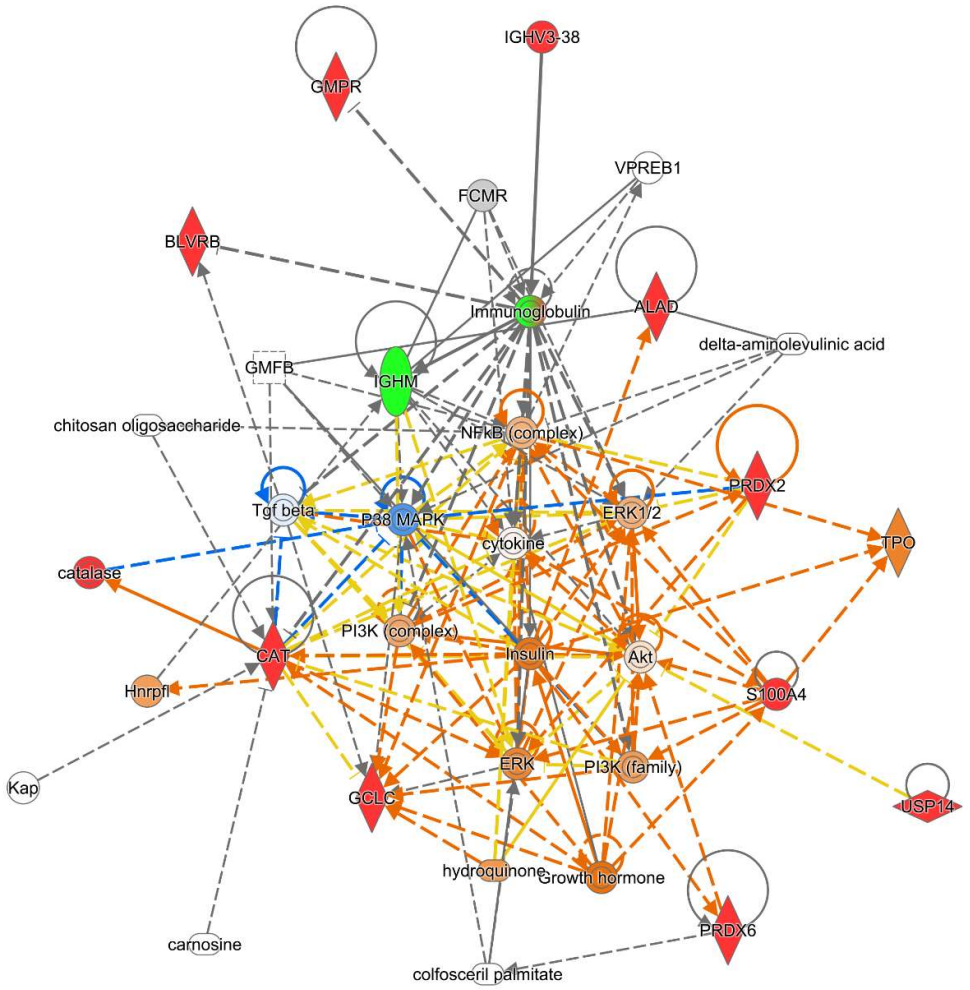

Figure S12. Quality control of CSF and serum proteomic data acquired by TMT-based LC-MS/MS analysis. The coefficient of variation (CV) between the pairing of 7 replicates for A) CSF and B) serum samples. Evaluation of batch effects using the pooled C) CSF and D) serum samples.

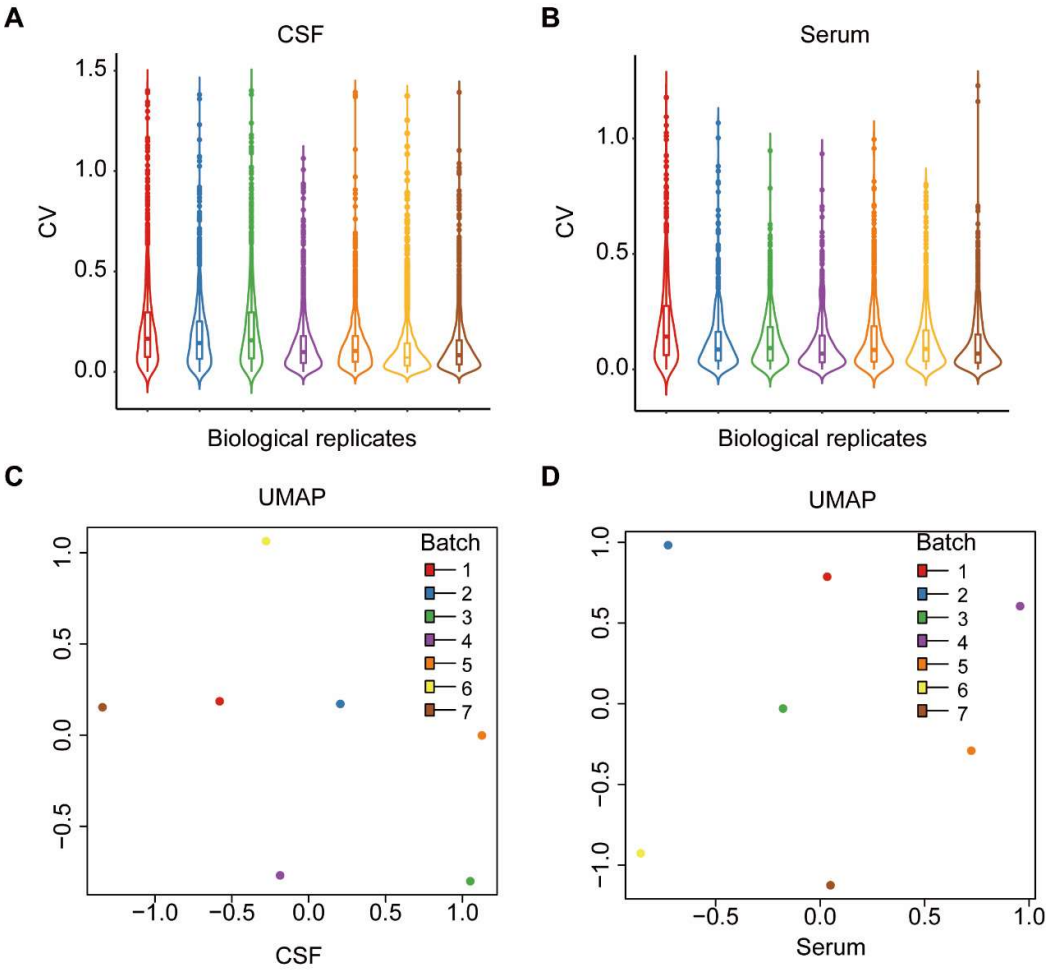

Figure S13. **Quality control of PRM proteome data**. The CVs of 11 and 16 technical replicates in **(A)** CSF and **(B)** serum samples, respectively. The Pearson correlation coefficient (r) for **(C)** 8 CSF pooled samples and **(D)** 10 serum pooled samples. Evaluation of batch effect using the pooled **(E)** CSF and **(F)** serum samples.